A NUMERICAL METHOD FOR THE COASTAL-TRAPPED WAVE PROBLEM

DAVID MICHAEL HOLLAND

A NUMERICAL METHOD FOR THE COASTAL-TRAPPED WAVE PROBLEM

BY

© *David Michael Holland*, B.Sc

A Thesis Submitted to the School of Graduate Studies in partial fulfillment of the requirements for the degree of Master of Science

Department of Physics
Memorial University of Newfoundland

February 1987

ISBN 0-315-37021-1

To Denise

Abstract

A numerical method is presented to solve the coastal-trapped wave (CTW) problem. The method is the explicitly shifted inverse power algorithm for the generalized eigenvalue problem. Problems non-linear in the eigenvalue, such as the dispersive baroclinic CTW problem, are addressed by expressing them as linear problems of expanded dimension. The novelty of the technique is its ability to compute complex eigenvalues directly.

In this thesis two applications of the method are presented. First, the effect of stratification on CTW's is investigated by determining their dispersion characteristics. These are computed for both real propagating and complex evanescent wavenumber solutions. Second, the influence of a mean alongshore current on CTW's is studied. The results are compared to observations made along the eastern Australian coast.

Acknowledgements

It is with deep appreciation that I acknowledge my research supervisor, Dr. I.T. Webster, for his invaluable assistance, his availability, and his insight into correcting many of the obstacles encountered along the way. I wish to thank the many staff of the Physics Department and Computing Services at Memorial University of Newfoundland who have assisted me with this project. I would also like to thank Dr. H.J. Freeland for providing experimental data.

This work was supported by a graduate scholarship from the Natural Sciences and Engineering Research Council of Canada.

Table of Contents

List of Figures

List of Tables

CHAPTER ONE

INTRODUCTION

A continental shelf is the main topographic feature found along the coastlines of the world. A shelf extends from the shoreline to a variable distance of between 10 and 300 km offshore where the water depth is of the order of 200 m. Beyond this distance exists the continental slope where the depth increases much more quickly to reach its average abyssal value of 4000 m. Because the shelf and slope are situated upon a rotating earth they act as a one-dimensional wave guide for the propagation of coastal-trapped waves (CTW's). The importance of CTW's is that they form the dominant circulation response of coastal waters to forcing by the atmosphere.

CTW phenomena have been investigated in detail since Hamon [1962] first detected a sea level signal of subinertial frequency propagating along the east coast of Australia. The first theoretical treatment of Hamon's observations was by Robinson [1964]. Using the depth-integrated linearized shallow water equations for a rotating ocean, wavelike solutions were obtained which propagated phase with the coast on the right (left) in the northern (southern) hemisphere. Later, Buchwald and Adams [1968] developed an analytical dispersion relation for these topographic Rossby waves which showed that they existed as discrete modes and that each mode had a subinertial cut-off frequency above which that mode could not exist. Brink [1980] showed that wavelike solutions do occur above the cut-off frequency, but that these modes were evanescent. The

evanescent modes differed from the usual propagating modes in that they did not transport energy in the alongshore direction and that their amplitude decayed in the alongshore direction.

The theory of CTW's was extended to include the more general feature of continuous density stratification by Wang and Mooers [1976]. They were able to show that stratification had the quantitative effect of increasing the modal phase speeds of CTW's. Later Chapman [1983] showed that sufficiently strong stratification led to the existence of propagating modes at all subinertial frequencies. It appears that stratification was able to produce a modal structure for the wave which was a hybrid of the internal Kelvin wave of a flat bottom ocean and the topographic Rossby wave of a sloping bottom.

The binding thread of the following work is the presentation of a numerical method for solving the CTW problem. The CTW problem is formulated as a generalized matrix eigenvalue problem which is non-linear in the eigenvalue. This is solved using an explicitly shifted inverse power algorithm. The special feature of the solution method is its ability to compute complex or evanescent modes directly as would result from the determination of evanescent solutions or of solutions including bottom friction. The first part of this thesis describes how stratification affects CTW propagation characteristics. The novelty of the work is its ability to show the behavior of the evanescent modes as a function of stratification.

There are many parametric variations to consider in the formulation of a complete theory of CTW dynamics such as the effect of the variation of Coriolis

force with latitude, irregular topography, bottom friction, wind forcing, and the presence of a mean alongshore current. With the exception of the alongshore current all of the above have been addressed in the literature [Mysak, 1980]. Accordingly in the second part of this thesis the effect of a mean current on CTW propagation is addressed. The numerical results obtained are compared to observations made during the Australian Coastal Experiment [Freeland *et al.*, 1986].

The outline of this thesis is as follows. The formulation of the CTW stratification problem is presented in Chapter two. The numerical method as applied to the stratification problem is presented in Chapter three, and the results of the effect of stratification on CTW's are presented in Chapter four. The CTW problem of Chapter two with the addition of a mean alongshore current is formulated in Chapter five. Finally Chapter six concludes the work by presenting the main results of the thesis.

CHAPTER TWO

EQUATIONS OF MOTION

The equations of motion governing the motion of fluid over a continental shelf are presented for the case in which the fluid has continuous vertical density stratification. The equations are reduced to a second order partial differential equation for pressure which is solved as a discrete eigenvalue problem.

2.1 Momentum Equations

Consider a hydrodynamic system consisting of an ocean over a continental shelf as depicted in Figure 2.1. A right-handed Cartesian coordinate system is chosen such that the x-axis refers to the offshore direction, the y-axis refers to the alongshore direction and the z-axis is vertically upwards. The topography varies only in the offshore direction and a straight coastline is assumed. The origin of the coordinate axes is the surface at the coast.

The equation governing the motion for a fluid element in an inviscid fluid on a rotating reference frame is [Gill, 1982]

$$\frac{D\vec{U}}{Dt} + 2\vec{\Omega}\times\vec{U} = -\frac{1}{\rho}\vec{\nabla}p - \vec{g}, \tag{2.1}$$

where $\vec{\Omega}$ is the angular velocity of the rotating frame, $\vec{U}$ is the velocity vector of

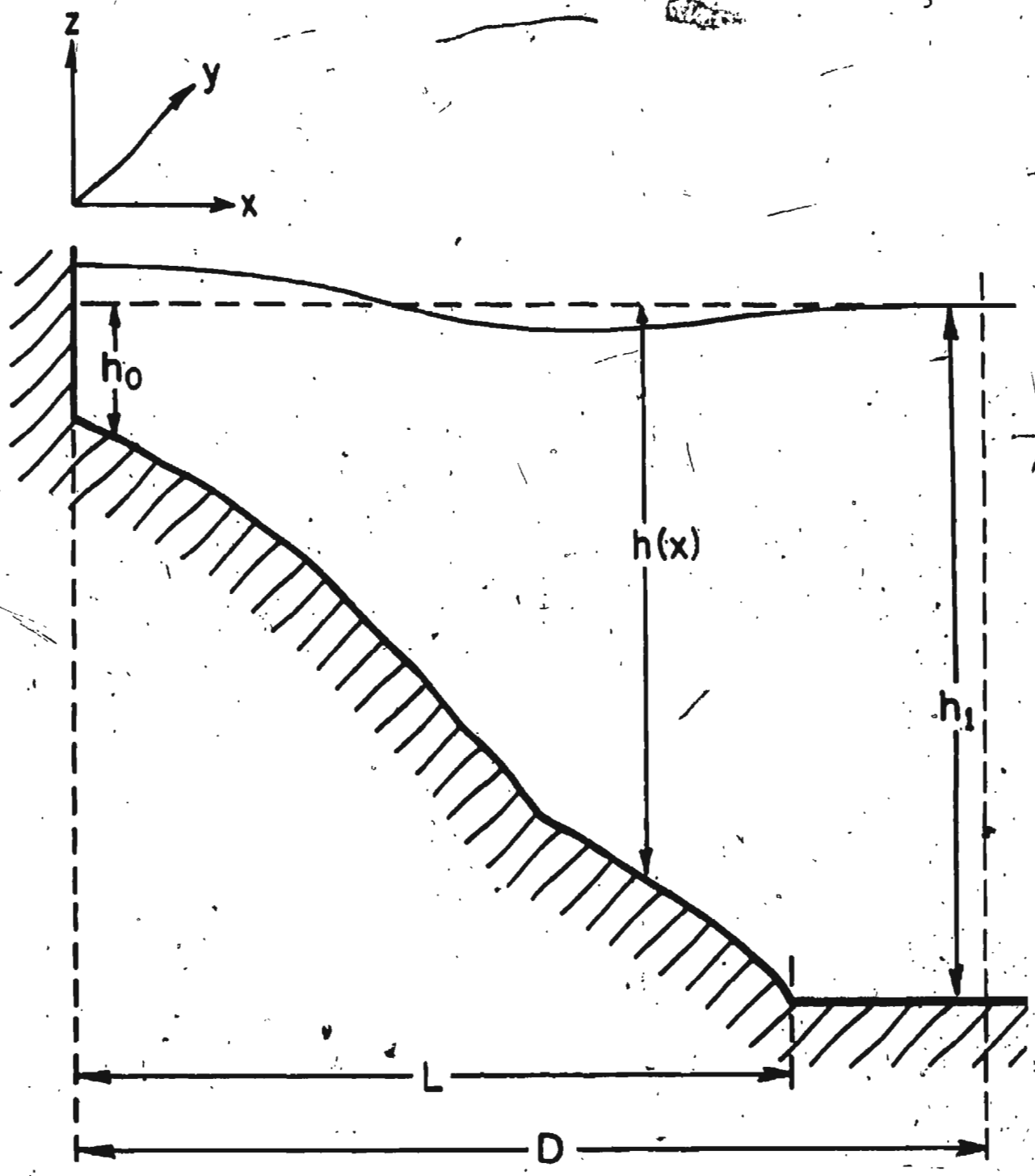

Figure 2.1 Schematic of a shelf profile showing the coordinate system.

the fluid element, ρ is the density, p is the pressure, and $\vec{g}$ is the gravitational acceleration. The quantities p and ρ have a mean state p_o and ρ_o respectively while $\vec{U}$ has a zero mean state. The presence of wavelike motion superimposed on the mean state causes a departure from the equilibrium states of p_o and ρ_o to

$$p = p_o(z) + p'(x,y,z,t), \tag{2.2a}$$

$$\rho = \rho_o(z) + \rho'(x,y,z,t), \tag{2.2b}$$

$$\vec{U} = \vec{U}'(x,y,z,t), \tag{2.2c}$$

where the perturbation pressure p', perturbation density ρ', and perturbation velocity $\vec{U}'$ have been introduced. Note that the perturbation velocity $\vec{U}'$ has three components namely u', v', and w' in the x, y, and z directions respectively.

The vector Equation (2.1) has three component equations [Pond and Pickard, 1983]

$$\frac{\partial u}{\partial t} + u\frac{\partial u}{\partial x} + v\frac{\partial u}{\partial y} + w\frac{\partial u}{\partial z} - 2\Omega\sin\phi v + 2\Omega\cos\phi w = \frac{-1}{\rho}\frac{\partial p}{\partial x}, \tag{2.3a}$$

$$\frac{\partial v}{\partial t} + u\frac{\partial v}{\partial x} + v\frac{\partial v}{\partial y} + w\frac{\partial v}{\partial z} + 2\Omega\sin\phi u = \frac{-1}{\rho}\frac{\partial p}{\partial y}, \tag{2.3b}$$

$$\frac{\partial w}{\partial t} + u\frac{\partial w}{\partial x} + v\frac{\partial w}{\partial y} + w\frac{\partial w}{\partial z} - 2\Omega\cos\phi u = \frac{-1}{\rho}\frac{\partial p}{\partial z} - g, \tag{2.3c}$$

which may be simplified as follows. Make the Boussinesq approximation that density variations ρ' about the mean ρ_o are unimportant except where they multiply the gravitational acceleration. The Coriolis term involving w is neglected in (2.3a) as it is small compared to the Coriolis term involving v. The Coriolis term in (2.3c) is also neglected as it is small with respect to the gravitational term.

For the Coriolis terms that remain introduce the Coriolis parameter as

$$f = 2\Omega\sin\phi, \tag{2.4}$$

where ϕ is the geographical latitude. In the formulation of the perturbation equations it is assumed that non-linear terms are negligible. Finally, for motions at sub-inertial frequencies the term $\frac{\partial w}{\partial t}$ in (2.3c) is negligible compared to the gravitational acceleration term.

The perturbation momentum equations for the horizontal motion then become from (2.3a) and (2.3b)

$$\frac{\partial u'}{\partial t} - fv' = \frac{-1}{\rho_o}\frac{\partial p'}{\partial x}, \tag{2.5a}$$

$$\frac{\partial v'}{\partial t} + fu' = \frac{-1}{\rho_o}\frac{\partial p'}{\partial y}. \tag{2.5b}$$

The vertical momentum Equation (2.3c) has a mean state which is the hydrostatic equation

$$-\rho_o g = \frac{\partial p_o}{\partial z}. \tag{2.6}$$

Subtracting this mean state from (2.3c), the resulting perturbation equation for the vertical momentum is

$$-\rho' g = \frac{\partial p'}{\partial z}. \tag{2.7}$$

2.2 Mass Conservation and Continuity Equation

The mass conservation equation, assuming no diffusion of density is [Gill, 1982]

$$\frac{1}{\rho}\frac{D\rho}{Dt} + \vec{\nabla}\cdot\vec{U} = 0. \tag{2.8}$$

Assuming the fluid is incompressible which is a good approximation for sea water requires

$$\vec{\nabla}\cdot\vec{U} = 0. \tag{2.9}$$

This may be expressed in Cartesian form as

$$\frac{\partial u'}{\partial x} + \frac{\partial v'}{\partial y} + \frac{\partial w'}{\partial z} = 0. \tag{2.10}$$

With (2.9), (2.8) becomes

$$\frac{D\rho}{Dt} = 0, \tag{2.11a}$$

or in expanded form

$$\frac{\partial \rho'}{\partial t} + u'\frac{\partial \rho'}{\partial x} + v'\frac{\partial \rho'}{\partial y} + w'\frac{\partial \rho_o}{\partial z} + w'\frac{\partial \rho'}{\partial z} = 0. \tag{2.11b}$$

Still further simplification is possible by neglecting non-linear terms yielding the equation

$$\frac{\partial \rho'}{\partial t} + w'\frac{\partial \rho_o}{\partial z} = 0. \tag{2.12}$$

Thus far we have a total of five Equations (2.5a), (2.5b), (2.7), (2.10), and (2.12) in five unknowns p', ρ', u', v', and w' which form a closed deterministic

system.

2.3 The Pressure Equation

We look for wavelike solutions of the set of five equations having the time and alongshore dependence $e^{i(ky + \omega t)}$ where k is the alongshore wavenumber and ω is the frequency of the wave motion. The perturbation quantities behave as

$$u'(x,y,z,t) = u''(x,z)e^{i(ky + \omega t)}, \tag{2.13a}$$

$$v'(x,y,z,t) = v''(x,z)e^{i(ky + \omega t)}, \tag{2.13b}$$

$$w'(x,y,z,t) = w''(x,z)e^{i(ky + \omega t)}, \tag{2.13c}$$

$$p'(x,y,z,t) = p''(x,z)e^{i(ky + \omega t)}, \tag{2.13d}$$

$$\rho'(x,y,z,t) = \rho''(x,z)e^{i(ky + \omega t)}. \tag{2.13e}$$

Upon substitution of (2.13) into (2.5a), (2.5b), (2.7), (2.10), and (2.12), we obtain the following equations having explicit x and z dependencies only

$$i\omega u'' - fv'' = \frac{-1}{\rho_o}\frac{\partial p''}{\partial x}, \tag{2.14a}$$

$$i\omega v'' + fu'' = \frac{-ik}{\rho_o}p'', \tag{2.14b}$$

$$-\rho''g = \frac{\partial p''}{\partial z}, \tag{2.14c}$$

$$i\omega\rho'' + w''\frac{\partial \rho_o}{\partial z} = 0, \tag{2.14d}$$

$$\frac{\partial u''}{\partial x} + ikv'' + \frac{\partial w''}{\partial z} = 0. \qquad (2.14e)$$

The system of Eqns. (2.14a-d) may be solved for the three velocity components as

$$u'' = -\frac{f}{(f^2 - \omega^2)\rho_o}\left[i\sigma\frac{\partial p''}{\partial x} + ikp''\right], \qquad (2.15a)$$

$$v'' = \frac{f}{(f^2 - \omega^2)\rho_o}\left[\frac{\partial p''}{\partial z} + k\sigma p''\right], \qquad (2.15b)$$

$$w'' = -\frac{f}{(f^2 - \omega^2)\rho_o}\left[\frac{i\sigma}{N^2}\frac{\partial p''}{\partial z}\right]. \qquad (2.15c)$$

In Equations (2.15) the non-dimensional buoyancy frequency and the non-dimensional wave frequency have been introduced, respectively as

$$N^2 = -\frac{g}{(f^2 - \omega^2)\rho_o}\frac{\partial \rho_o}{\partial z}, \qquad (2.16a)$$

and

$$\sigma = \frac{\omega}{f}. \qquad (2.16b)$$

A governing equation in pressure $p''(x,z)$ in the interior of the fluid is obtained by substituting the expressions for velocity components (2.15) into the incompressibility Equation (2.14e) to yield

$$\frac{\partial^2 p''}{\partial z^2} - k^2 p'' + \frac{1}{N^2}\frac{\partial^2 p''}{\partial x^2} = 0. \qquad (2.17a)$$

The derivation of the above was carried out under the assumptions that both the

buoyancy frequency and the Coriolis frequency are constant.

The boundary equations in $p''(x,z)$ are obtained by considering the flow properties at each boundary (see Figure 2.1). The basic condition is that of no flow normal to each boundary except at the offshore boundary. At the coast the boundary is vertical [Mitchum and Clarke, 1986] so $u'' = 0$ and hence

$$\sigma\frac{\partial p''}{\partial x} + kp'' = 0. \tag{2.17b}$$

Along the sloping bottom of the shelf upon which $z = -h(x)$, where $h(x)$ is the fluid depth as a function of offshore distance x, the flow condition is $u''\frac{\partial h}{\partial x} + w'' = 0$ requiring that

$$\sigma\frac{\partial p''}{\partial x} + kp'' + \frac{\sigma}{N^2\frac{\partial h}{\partial x}}\frac{\partial p''}{\partial z} = 0. \tag{2.17c}$$

Where the bottom is flat $\frac{\partial h}{\partial x} = 0$ so the above condition is simplified to $w'' = 0$ yielding

$$\frac{\partial p''}{\partial z} = 0. \tag{2.17d}$$

Applying the rigid-lid approximation along the surface at $z = 0$ leads to $w'' = 0$ there so that Equation (2.17d) applies at the surface as well. The offshore condition is that the oceanic response be trapped at the coast so that $p'' \to 0$ as $z \to \infty$. As this condition is impractical to implement in a numerical scheme, the domain is restricted to an offshore distance of D some distance past the seaward edge of the shelf at L (see Figure 2.1). An appropriate choice for D is approximately 1.5 times L [Chapman, 1983]. There the condition that the gradient of normal

velocity must vanish is applied [Brink, 1982] which is $\frac{\partial u''}{\partial z} = 0$ so

$$\sigma \frac{\partial^2 p''}{\partial z^2} + k \frac{\partial p''}{\partial z} = 0. \tag{2.17e}$$

2.4 The Eigenvalue Problem

The Equations (2.17) may be re-expressed by collecting all terms involving k to the right hand side of each equation and omitting the double prime notation to yield

in the interior

$$\frac{\partial^2 p}{\partial z^2} + \frac{1}{N^2} \frac{\partial^2 p}{\partial z^2} = k^2 p\,, \tag{2.18a}$$

at $z = 0$

$$\sigma \frac{\partial p}{\partial z} = -kp\,, \tag{2.18b}$$

along $z = -h(x)$ for $z \leq L$

$$\sigma \frac{\partial p}{\partial z} + \frac{\sigma}{N^2 \frac{\partial h}{\partial z}} \frac{\partial p}{\partial z} = -kp \tag{2.18c}$$

at $z = 0$ and at $z = -h(x)$ for $z > L$

$$\frac{\partial p}{\partial z} = 0, \tag{2.18d}$$

and finally at $z = D$

$$\sigma \frac{\partial^2 p}{\partial x^2} = -k \frac{\partial p}{\partial z}. \tag{2.18c}$$

For fixed σ these equations constitute an eigenvalue problem in the eigenvalue k, the alongshore wavenumber. Since it is quadratic in the eigenvalue a special technique is employed for its solution.

CHAPTER THREE

NUMERICAL METHODS

The solution to the partial differential Equation (2.18) is sought over the irregular two-dimensional shelf domain. It is convenient to transform the domain into a rectangular domain by a vertically stretched coordinate transformation. The equations are then discretized and are formed into a matrix eigenvalue problem non-linear in the eigenvalue. The problem is linearized at the cost of increasing the dimension of the solution space. The system is then solved using an iterative procedure called the inverse power algorithm whereby the perturbation pressure at each grid point is obtained as well as the value of the alongshore wavenumber k.

3.1 Coordinate Transformation

The motivation for using a coordinate transformation is that a solution to (2.18) is more easily obtained in a rectangular domain. To carry out the transformation it is necessary to derive expressions which relate the derivative functions in the irregular and the rectangular domains. A mapping from the irregular domain of Figure 2.1 to a rectangular domain is a vertically stretched coordinate transformation from (x, z) space to (x', z') space according to

$$x' = x, \tag{3.1a}$$

$$z' = T(x)z, \tag{3.1b}$$

where

$$T(x) = \frac{1}{h(x)}. \tag{3.2}$$

In transformed space, the depth z' now goes from zero at the surface to a value of one at the bottom irrespective of horizontal position along the shelf bottom or flat bottom.

The details of the transformation are presented in Appendix A. The following relate derivatives in the irregular domain to those in the rectangular domain

$$\frac{\partial p}{\partial x} = \frac{\partial p}{\partial x'} + \frac{\partial T}{\partial x'}\frac{z'}{T}\frac{\partial p}{\partial z'}, \tag{3.3a}$$

$$\frac{\partial p}{\partial z} = T\frac{\partial p}{\partial z'}, \tag{3.3b}$$

$$\frac{\partial^2 p}{\partial x^2} = \frac{\partial^2 p}{\partial x'^2} + 2\frac{\partial T}{\partial x'}\frac{z'}{T}\frac{\partial^2 p}{\partial x' \partial z'} + \left(\frac{\partial T}{\partial x'}\frac{z'}{T}\right)^2\frac{\partial^2 p}{\partial z'^2} + \frac{\partial^2 T}{\partial x'^2}\frac{z'}{T}\frac{\partial p}{\partial z'}, \tag{3.3c}$$

$$\frac{\partial^2 p}{\partial z^2} = T^2\frac{\partial^2 p}{\partial z'^2}. \tag{3.3d}$$

Substituting these expressions into Equations (2.18) results in the following transformed equations

interior

$$\frac{\partial^2 p}{\partial x'^2} + \left[\left(\frac{\partial T}{\partial x'}\frac{z'}{T}\right)^2 + \frac{T^2}{N^2}\right]\frac{\partial^2 p}{\partial z'^2} + \left(2\frac{\partial T}{\partial x'}\frac{z'}{T}\right)\frac{\partial^2 p}{\partial x' \partial z'} + \tag{3.4a}$$

$$\left(\frac{\partial^2 T}{\partial x'^2}\frac{z'}{T}\right)\frac{\partial p}{\partial z'} = k^2 p,$$

coast

$$\sigma\frac{\partial p}{\partial x'} + \sigma\frac{\partial T}{\partial x'}\frac{z'}{T}\frac{\partial p}{\partial z'} = -kp, \tag{3.4b}$$

sloping bottom

$$\sigma\frac{\partial p}{\partial x'} + \sigma\left[\frac{\partial T}{\partial x'}\frac{z'}{T} + \frac{T}{N^2}\frac{\partial h}{\partial x'}\right]\frac{\partial p}{\partial z'} = -kp, \tag{3.4c}$$

surface or flat bottom

$$\frac{\partial p}{\partial z'} = 0, \tag{3.4d}$$

offshore

$$\sigma\frac{\partial^2 p}{\partial z'^2} = -k\frac{\partial p}{\partial z'}. \tag{3.4e}$$

Simplification of the transformations (3.3) are possible in certain regions of the domain. Anywhere the ocean bottom is flat $\frac{\partial h}{\partial x}$ will be zero and consequently by (3.2) both $\frac{\partial T}{\partial x'}$ and $\frac{\partial^2 T}{\partial x'^2}$ will be zero. Terms involving these quantities may be ignored when Equations (3.4) are evaluated over any portion of the domain which has a flat bottom. In particular Equation (3.4e) was derived under the assumption that the ocean has a flat bottom in the region where the offshore boundary condition is applied. An additional simplification is that by virtue of the choice of the origin of the (x', z') coordinate system at the surface of the

coastal boundary, then z' is zero everywhere along the surface boundary. This implies all terms involving z' are dropped when Equations (3.4) are applied at the surface. Such simplifications lead to computational savings.

3.2 Finite Difference Forms

The next step in the scheme is to transform the continuous Equations (3.4) into a set of discrete equations. The domain is to be expressed as a grid (see Figure 3.1); there will be one discrete equation for each grid point. The prime superscripts on x and z are now dropped as all references to a coordinate system are henceforth to the transformed one. A rectangular mesh system is set up where each point is indexed by a pair of subscripts (i, j), the i referring to the x direction and the j referring to the z direction. The mesh spacing in the x direction is Δx, and in the z direction it is Δz. A centered finite difference scheme is used. The basis for this choice is that the pressure at a point in the domain is assumed to have continuous x and z derivatives and thereby can be expanded about that point in a Taylor's series. For details of the finite difference scheme see Appendix B. The continuum derivative at a point thereby becomes an approximation involving the point itself and its nine nearest neighbours. The discrete derivatives are [Roache, 1985]

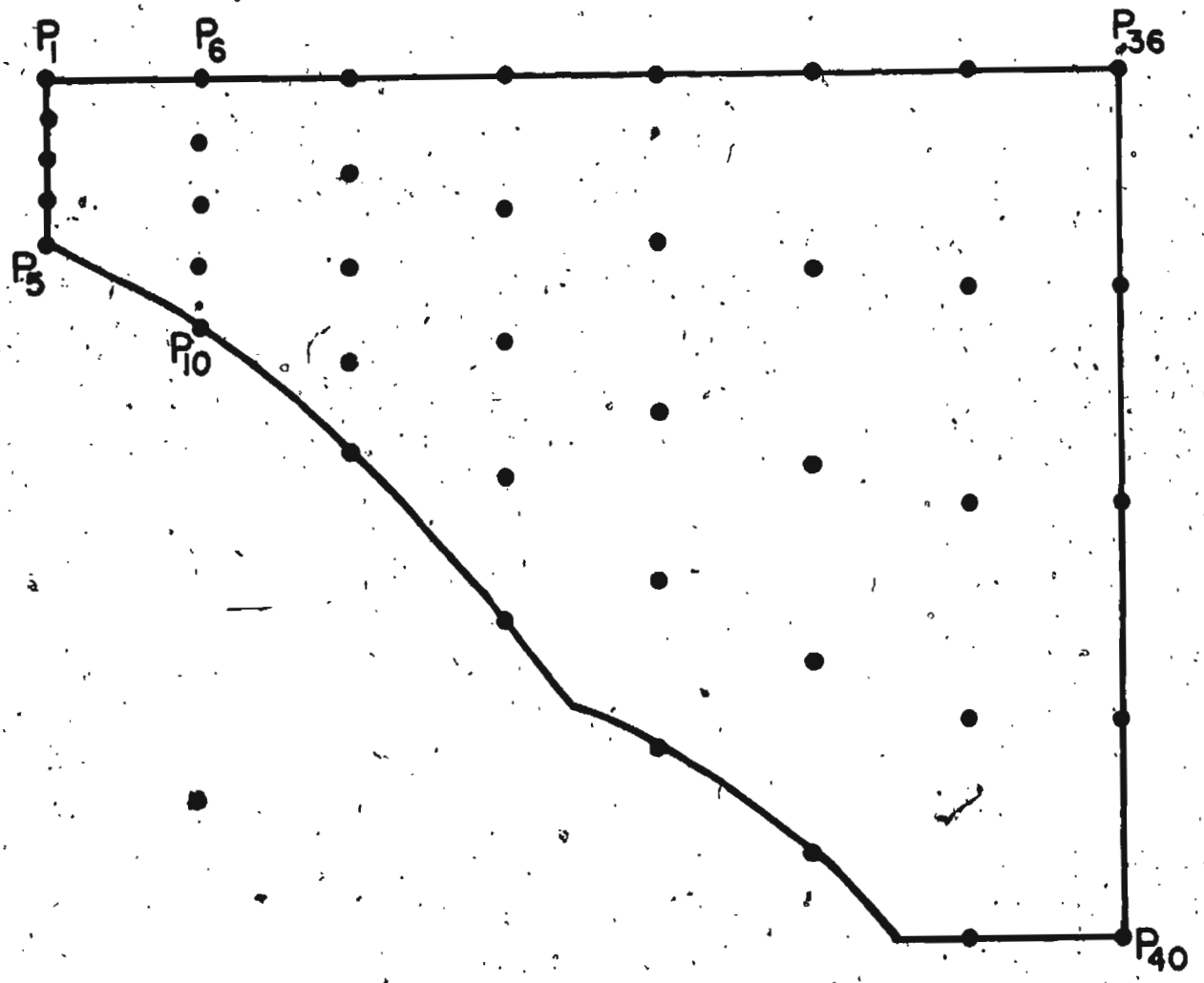

Figure 3.1 An example of the numerical discretization of the perturbation pressure over the shelf profile.

$$\frac{\partial p}{\partial x} = \frac{p_{i+1,j} - p_{i-1,j}}{2\Delta x}, \tag{3.5a}$$

$$\frac{\partial p}{\partial z} = \frac{p_{i,j+1} - p_{i,j-1}}{2\Delta z}, \tag{3.5b}$$

$$\frac{\partial^2 p}{\partial x^2} = \frac{p_{i+1,j} - 2p_{i,j} + p_{i-1,j}}{\Delta x^2}, \tag{3.5c}$$

$$\frac{\partial^2 p}{\partial z^2} = \frac{p_{i,j+1} - 2p_{i,j} + p_{i,j-1}}{\Delta z^2}, \tag{3.5d}$$

$$\frac{\partial^2 p}{\partial x\,\partial z} = \frac{p_{i+1,j+1} + p_{i-1,j-1} - p_{i+1,j-1} - p_{i-1,j+1}}{4\Delta x\,\Delta z}. \tag{3.5e}$$

Substitution of (3.5) into the set of Equations (3.4) yields the following equations

interior:

$$\left(\frac{\partial T}{\partial x}\frac{z}{2T\,\Delta x\,\Delta z}\right)p_{i+1,j+1} + \left(\frac{1}{\Delta x^2}\right)p_{i+1,j} - \left(\frac{\partial T}{\partial x}\frac{z}{2T\,\Delta x\,\Delta z}\right)p_{i+1,j-1} \tag{3.6a}$$

$$+ \left(\left(\frac{\partial T}{\partial x}\frac{z}{\Delta z T}\right)^2 - \frac{T^2}{N^2\Delta z^2} + \frac{\frac{\partial^2 T}{\partial x^2}}{2\Delta z T}\right)p_{i,j+1}$$

$$+ \left(\frac{-2}{\Delta x^2} - \left(2\frac{\partial T}{\partial x}\frac{z}{\Delta z^2 T}\right)^2 - 2\frac{T^2}{N^2\Delta z^2}\right)p_{i,j}$$

$$+ \left(\left(\frac{\partial T}{\partial x}\frac{z}{\Delta z T}\right)^2 - \frac{T^2}{N^2\Delta z^2} - \frac{\frac{\partial^2 T}{\partial x^2}}{2\Delta z T}\right)p_{i,j-1}$$

$$- \left(\frac{\partial T}{\partial x}\frac{z}{2T\,\Delta x\,\Delta z}\right)p_{i-1,j+1} + \left(\frac{1}{\Delta x^2}\right)p_{i-1,j} + \left(\frac{\partial T}{\partial x}\frac{z}{2T\,\Delta x\,\Delta z}\right)p_{i-1,j-1}$$

$$= k^2 p_{i,j},$$

coast

$$\left(\frac{\sigma}{2\Delta x}\right) p_{i+1,j} + \left(\sigma \frac{\partial T}{\partial x} \frac{z}{2\Delta z T}\right) p_{i,j+1} - \tag{3.6b}$$

$$\left(\sigma \frac{\partial T}{\partial x} \frac{z}{2\Delta z T}\right) p_{i,j-1} - \left(\frac{\sigma}{2\Delta x}\right) p_{i-1,j} = -k p_{i,j},$$

shelf bottom

$$\left(\frac{\sigma}{2\Delta x}\right) p_{i+1,j} + \left(\sigma \frac{\partial T}{\partial x} \frac{z}{2\Delta z T} + \sigma \frac{T}{2\Delta z N^2 \frac{\partial h}{\partial x}}\right) p_{i,j+1} - \tag{3.6c}$$

$$\left(\sigma \frac{\partial T}{\partial x} \frac{z}{2\Delta z T} + \sigma \frac{T}{2\Delta z N^2 \frac{\partial h}{\partial x}}\right) p_{i,j-1} - \left(\frac{\sigma}{2\Delta x}\right) p_{i-1,j} = -k p_{i,j},$$

surface and flat bottom

$$p_{i,j+1} - p_{i,j-1} = 0, \tag{3.6d}$$

offshore

$$\left(\frac{\sigma}{\Delta x^2}\right) p_{i+1,j} - \left(2\frac{\sigma}{\Delta x^2}\right) p_{i,j} + \left(\frac{\sigma}{\Delta x^2}\right) p_{i-1,j} = \tag{3.6e}$$

$$-k\left[\left(\frac{1}{2\Delta x}\right) p_{i+1,j} - \left(\frac{1}{2\Delta x}\right) p_{i+1,j}\right].$$

The Equations (3.6) form a system of equations in which the unknowns are the pressures $p_{i,j}$ at each grid point. The equation for the interior of the fluid (3.6a) is applied at each point in the interior of the domain and at each point along the boundary. The interior Equation (3.6a) is applied at a total of $N = nx \times nz$ points where nx is the number of points in the horizontal and nz is

the number in the vertical direction. The interior equation applied at a point along the boundary of the domain will involve points exterior to the domain. The appropriate boundary Equation (3.6b - 3.6e) is used to eliminate the unknown exterior points from the interior equation.

3.3 Matrix Formulation

In the domain there are N points at which the pressure is to be solved for. An N dimensional vector $\hat{P}$ is constructed by considering all the points in the first column for which $i = 1$ (i.e. at the coast), from the surface to the bottom which has $j = 1, \cdots, nz$ points and then adding on each consecutive column of points in the direction of the offshore corresponding to $i = 2, \cdots, nz$ until $\hat{P}$ references every point in the domain. Equations (3.6) can be written as

$$\mathbf{A}\hat{P} = k\mathbf{B}\hat{P} + k^2\mathbf{C}\hat{P}, \tag{3.7}$$

where **A**, **B**, **C** are linear matrix operators. As each row of the matrices **A**, **B**, and **C** are multiplied by $\hat{P}$ in the operation symbolized by (3.7) then each row represents an equation at one unique point in the domain. There are a total of N equations and hence **A**, **B**, and **C** are each N×N dimensional.

The non-linear problem (3.7) can be expressed as a linear problem with the substitution

$$\hat{Q} = k\hat{P}, \tag{3.8}$$

into the second term on the right-hand side of (3.7) where the vector $\hat{Q}$ is N

dimensional. This equation becomes

$$\mathbf{A}\dot{P} = k\mathbf{B}\ddot{P} + k\mathbf{C}\dot{Q}. \tag{3.9}$$

The system of Equations (3.8) and (3.9) then form a problem of dimension 2N

$$\begin{pmatrix} \mathbf{A} & \mathbf{O} \\ \mathbf{O} & \mathbf{I} \end{pmatrix} \begin{bmatrix} \dot{P} \\ \dot{Q} \end{bmatrix} = k \begin{pmatrix} \mathbf{B} & \mathbf{C} \\ \mathbf{I} & \mathbf{O} \end{pmatrix} \begin{bmatrix} \dot{P} \\ \dot{Q} \end{bmatrix}, \tag{3.10}$$

where I is the identity matrix and O is the null matrix. Both I and O are N×N dimensional.

Instead of solving (3.10) directly it is desireable to introduce an explicit shift s which is an estimate of k used to improve solution convergence as well as to isolate a particular solution [Stewart, 1973]. The vector

$$s \begin{pmatrix} \mathbf{B} & \mathbf{C} \\ \mathbf{I} & \mathbf{O} \end{pmatrix} \begin{bmatrix} \dot{P} \\ \dot{Q} \end{bmatrix}, \tag{3.11}$$

is subtracted from both sides of (3.10) to yield

$$\begin{pmatrix} \mathbf{A} - s\mathbf{B} & -s\mathbf{C} \\ -s\mathbf{I} & \mathbf{I} \end{pmatrix} \begin{bmatrix} \dot{P} \\ \dot{Q} \end{bmatrix} = (k - s) \begin{pmatrix} \mathbf{B} & \mathbf{C} \\ \mathbf{I} & \mathbf{O} \end{pmatrix} \begin{bmatrix} \dot{P} \\ \dot{Q} \end{bmatrix}. \tag{3.12}$$

Rearrangement of this vector equation yields

$$\begin{pmatrix} \mathbf{A} - s\mathbf{B} & -s\mathbf{C} \\ -s\mathbf{I} & \mathbf{I} \end{pmatrix}^{-1} \begin{pmatrix} \mathbf{B} & \mathbf{C} \\ \mathbf{I} & \mathbf{O} \end{pmatrix} \begin{bmatrix} \dot{P} \\ \dot{Q} \end{bmatrix} = \frac{1}{k - s} \begin{bmatrix} \dot{P} \\ \dot{Q} \end{bmatrix}. \tag{3.13}$$

We note that

$$\begin{pmatrix} \mathbf{A} - s\mathbf{B} & -s\mathbf{C} \\ -s\mathbf{I} & \mathbf{I} \end{pmatrix} \begin{bmatrix} \mathbf{D}^{-1}\mathbf{I} & s\mathbf{D}^{-1}\mathbf{C} \\ s\mathbf{D}^{-1}\mathbf{I} & \mathbf{D}^{-1}(\mathbf{A} - s\mathbf{B}) \end{bmatrix} = \begin{pmatrix} \mathbf{I} & \mathbf{O} \\ \mathbf{O} & \mathbf{I} \end{pmatrix}, \tag{3.14}$$

where

$$\mathbf{D} = \mathbf{A} - s\mathbf{B} - s^2\mathbf{C}. \tag{3.15}$$

From the definition of the inverse of a matrix it follows that

$$\begin{pmatrix} \mathbf{A} - s\mathbf{B} & -s\mathbf{C} \\ -s\mathbf{I} & \mathbf{I} \end{pmatrix}^{-1} = \begin{bmatrix} \mathbf{D}^{-1}\mathbf{I} & s\mathbf{D}^{-1}\mathbf{C} \\ s\mathbf{D}^{-1}\mathbf{I} & \mathbf{D}^{-1}(\mathbf{A} - s\mathbf{B}) \end{bmatrix}. \tag{3.16}$$

After substitution of this inverse expansion into (3.13), the vector equation can be multiplied out to yield

$$\begin{bmatrix} \mathbf{D}^{-1}(\mathbf{B} + s\mathbf{C}) & \mathbf{D}^{-1}\mathbf{C} \\ \mathbf{D}^{-1}\mathbf{A} & s\mathbf{D}^{-1}\mathbf{C} \end{bmatrix} \begin{bmatrix} \hat{P} \\ \hat{Q} \end{bmatrix} = \frac{1}{k - s} \begin{bmatrix} \hat{P} \\ \hat{Q} \end{bmatrix}. \tag{3.17}$$

The Equation (3.17) has the standard form of a discrete eigenvalue problem

$$\mathbf{M}\hat{\xi} = \lambda\hat{\xi}, \tag{3.18}$$

where $\mathbf{M}$ is the $2N \times 2N$ dimensional matrix

$$\mathbf{M} = \begin{bmatrix} \mathbf{D}^{-1}(\mathbf{B} + s\mathbf{C}) & \mathbf{D}^{-1}\mathbf{C} \\ \mathbf{D}^{-1}\mathbf{A} & s\mathbf{D}^{-1}\mathbf{C} \end{bmatrix}, \tag{3.19}$$

$\hat{\xi}$ is the $2N$ dimensional vector

$$\hat{\xi} = \begin{bmatrix} \hat{P} \\ \hat{Q} \end{bmatrix}, \tag{3.20}$$

and $\lambda = \dfrac{1}{k - s}$ is the eigenvalue.

The eigenvector corresponding to the eigenvalue of largest absolute value, say λ_1, which in turn corresponds to the $k - s$ of smallest absolute value can be determined by application of the inverse power algorithm. To understand how the algorithm leads to a solution eigenvector $\hat{\xi}_1$ of (3.18) with eigenvalue λ_1 from some initial and arbitrary vector $\hat{\xi}^0$ it is necessary to assume that $\mathbf{M}$ has a complete set of eigenvectors $\hat{\xi}_1, \hat{\xi}_2, \ldots, \hat{\xi}_{2N}$ which have corresponding eigenvalues satis-

fying

$$|\lambda_1| > |\lambda_2| \geq \cdots \geq |\lambda_{2N}|. \tag{3.21}$$

Since the set of eigenvectors form a basis for the space spanned by **M** then any vector $\hat{\xi}^o$ may be expressed in the form

$$\hat{\xi}^o = \gamma_1\hat{\xi}_1 + \gamma_2\hat{\xi}_2 + \cdots + \gamma_{2N}\hat{\xi}_{2N}, \tag{3.22}$$

where the γ_i are some scalars for $i = 1, 2, \ldots, 2N$. It is evident that repeated application of **M** on $\hat{\xi}^o$ say ν times will lead to

$$\mathbf{M}^\nu\hat{\xi}^o = \lambda_1{}^\nu\gamma_1\hat{\xi}_1 + \lambda_2{}^\nu\gamma_2\hat{\xi}_2 + \cdots + \lambda_{2N}{}^\nu\gamma_{2N}\hat{\xi}_{2N}. \tag{3.23}$$

A particular eigenvalue k_1 of (3.10) can be singled out for computation by choosing an s in the neighbourhood of k_1 so that λ_1 will be large and (3.21) will be satisfied. The rate of convergence of (3.23) on the eigenvector of largest eigenvalue depends in part on the relative magnitudes of the largest eigenvalues. Assuming λ_2 is the second largest eigenvalue (in magnitude) then convergence on λ_1 tends to be quick provided $|\lambda_1| >> |\lambda_2|$.

If ν is large enough and (3.21) is valid then the eigenvalue λ_1 will dominate so that to an arbitrarily good degree of approximation

$$\mathbf{M}^\nu\hat{\xi}^o = \hat{\xi}_1{}^\nu \approx \lambda_1{}^\nu\gamma_1\hat{\xi}_1, \tag{3.24}$$

where $\hat{\xi}_1{}^\nu$ is the estimated $\hat{\xi}_1$ after the ν^{th} iteration.

The manner in which the solution technique works is that we assume that after iteration ν we have computed $\hat{\xi}_1{}^\nu$. Note that to get the iteration procedure started we picked $\hat{\xi}^o$ arbitrarily. The improved solution at iteration $\nu + 1$ is

determined by a single application of **M** since

$$\mathbf{M}\hat{\xi}_1^{\nu} = \hat{\xi}_1^{\nu+1}. \tag{3.25}$$

This procedure is continued until convergence to a single eigenvector is obtained. This eigenvector is identified as $\hat{\xi}_1$.

Once the eigenvector $\hat{\xi}_1$ is known then the eigenvalue λ_1 is immediately known by one more application of **M** as in

$$\mathbf{M}\hat{\xi}_1 = \lambda_1\hat{\xi}_1. \tag{3.26}$$

Recalling the definition of $\hat{\xi}$ from (3.20) it is possible to rewrite (3.25) as two component equations for the original unknowns $\hat{P}^{\nu+1}$ and $\hat{Q}^{\nu+1}$ as

$$\hat{P}^{\nu+1} = \mathbf{D}^{-1}(\mathbf{B} + s\,\mathbf{C})\hat{P}^{\nu} + \mathbf{D}^{-1}\mathbf{C}\hat{Q}^{\nu}, \tag{3.27a}$$

and

$$\hat{Q}^{\nu+1} = s\hat{R}^{\nu+1} + \hat{P}^{\nu}. \tag{3.27b}$$

where $\hat{P}^{\nu}$ and $\hat{Q}^{\nu}$ are known from the previous iteration. There is a difficulty with (3.27) in that it requires the inversion of **D** an N×N matrix where N is of the order of several hundred points. It is therefore impractical to attempt a solution of (3.24) by inverting **D** directly.

3.4 Alternate Formulation

Instead of solving the eigenvalue problem (3.27) with N×N dimensional matrices the problem can be solved by dealing with nz sets of matrices of size $nz \times nz$. The vector $\hat{P}$ may be broken up into a set of $i = 1, \ldots, nz$ column vectors $\hat{p}_i$ each of dimension nz, with each subvector $\hat{p}$ spanning from the ocean bottom to the surface. The equation at point (i,j) involves points lying within the columns $i-1$, i, and $i+1$ only. This suggests a method of reformulating the Equations (3.6) in matrix notation in analogy with (3.27) as

$$\left(\mathbf{a}^+_i - s\,\mathbf{b}^+_i - s^2\mathbf{c}^+_i\right)\hat{p}_{i+1}{}^{\nu+1} + \left(\mathbf{a}^o_i - s\,\mathbf{b}^o_i - s^2\mathbf{c}^o_i\right)\hat{p}_i{}^{\nu+1} + \tag{3.28a}$$

$$\left(\mathbf{a}^-_i - s\,\mathbf{b}^-_i - s^2\mathbf{c}^-_i\right)\hat{p}_{i-1}{}^{\nu+1} = \left(\mathbf{b}^+_i + s\,\mathbf{c}^+_i\right)\hat{p}_{i+1}{}^{\nu} + \mathbf{c}^+_i\,\hat{q}_{i+1}{}^{\nu} +$$

$$\left(\mathbf{b}^o_i + s\,\mathbf{c}^o_i\right)\hat{p}_i{}^{\nu} + \mathbf{c}^o_i\,\hat{q}_i{}^{\nu} + \left(\mathbf{b}^-_i + s\,\mathbf{c}^-_i\right)\hat{p}_{i-1}{}^{\nu} + \mathbf{c}^-_i\,\hat{q}_{i-1}{}^{\nu},$$

and

$$\hat{q}_i{}^{\nu+1} = s\hat{p}_i{}^{\nu+1} + \hat{p}_i{}^{\nu}, \tag{3.28b}$$

where all matrices are of dimension $nz \times nz$ and all vectors are of dimension nz. The manner in which the submatrices $\mathbf{a}^+_i$, $\mathbf{a}^o_i$, $\mathbf{a}^-_i$ are derived from the matrix A, the $\mathbf{b}^+_i$, $\mathbf{b}^o_i$, $\mathbf{b}^-_i$ from B, and the $\mathbf{c}^+_i$, $\mathbf{c}^o_i$, $\mathbf{c}^-_i$ from C is illustrated in Figure 3.2. Also depicted is the relation between the subvectors $\hat{p}_i$ and the vector $\hat{P}$. Thus the nz set of Equations (3.28) are equivalent to (3.27) and have the advantage of being more manageable numerically.

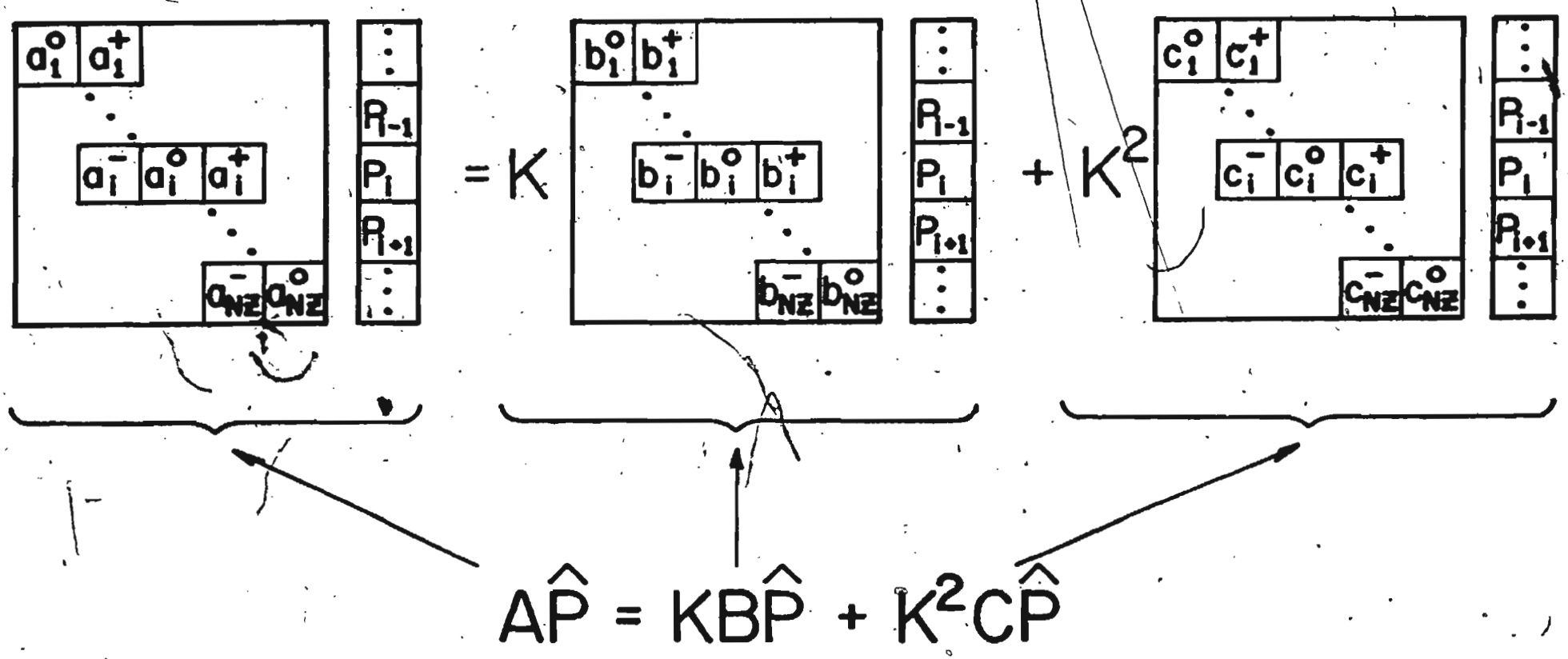

Figure 3.2 Diagrammatic relation between formulation of eigenvalue problem and the alternate submatrix formulation.

On each iteration, the solution vectors of the perturbation pressures are determined for each of the nz columns of the domain. The following is an explanation of exactly how the perturbation pressures for each column are determined at the $\nu+1$ iteration by using a modified form of Gaussian elimination. Consider the nz set of equations of the form (3.28). In general we relate two adjacent columns in the domain using an expression of the form [Lindzen and Kuo, 1969]

$$\hat{p}_{i-1}{}^{\nu+1} = \hat{\alpha}_{i-1}\hat{p}_i{}^{\nu+1} + \hat{\beta}_{i-1}, \tag{3.29}$$

where $\hat{\alpha}_i$ is a $nz \times nz$ matrix and $\hat{\beta}_i$ is a nz dimensional vector.

For (3.28a) at the coastal boundary ($i = 1$) we have

$$(\mathbf{a}^+{}_1 - s\,\mathbf{b}^+{}_1 - s^2\mathbf{c}^+{}_1)\hat{p}_2{}^{\nu+1} + (\mathbf{a}^o{}_1 - s\,\mathbf{b}^o{}_1 - s^2\mathbf{c}^o{}_1)\hat{p}_1{}^{\nu+1} = \tag{3.30}$$

$$(\mathbf{b}^+{}_1 + s\,\mathbf{c}^+{}_1)\hat{p}_2{}^{\nu} + \mathbf{c}^+{}_1\hat{q}_2{}^{\nu} + (\mathbf{b}^o{}_1 + s\,\mathbf{c}^o{}_1)\hat{p}_1{}^{\nu} + \mathbf{c}^o{}_1\hat{q}_1{}^{\nu}.$$

There is no reference to column $i-1$, that is column 0, as it was implicitly eliminated in the formulation of (3.28). The form of (3.29) at the coastal boundary is

$$\hat{p}_1{}^{\nu+1} = \alpha_1\hat{p}_2{}^{\nu+1} + \hat{\beta}_1. \tag{3.31}$$

Inspection of (3.30) leads to

$$\alpha_1 = -\frac{(\mathbf{a}^+{}_1 - s\,\mathbf{b}^+{}_1 - s^2\mathbf{c}^+{}_1)}{(\mathbf{a}^o{}_1 - s\,\mathbf{b}^o{}_1 - s^2\mathbf{c}^o{}_1)}, \tag{3.32a}$$

$$\hat{\beta}_1 = \frac{(\mathbf{b}^+{}_1 + s\,\mathbf{c}^+{}_1)\hat{p}_2{}^{\nu} + \mathbf{c}^+{}_1\hat{q}_2{}^{\nu} + (\mathbf{b}^o{}_1 + s\,\mathbf{c}^o{}_1)\hat{p}_1{}^{\nu} + \mathbf{c}^o{}_1\hat{q}_1{}^{\nu}}{(\mathbf{a}^o{}_1 - s\,\mathbf{b}^o{}_1 - s^2\mathbf{c}^o{}_1)}. \tag{3.32b}$$

A matrix division convention for (3.32) and subsequent matrix quotients is

introduced such that

$$\frac{\mathbf{A}}{\mathbf{B}} = \mathbf{B}^{-1}\mathbf{A}, \tag{3.33}$$

for arbitrary matrices **A** and **B**.

Next for columns from $i = 2, \cdots, nz$ the relations for α_i and $\hat{\beta}_i$ are derived from substituting (3.29) into the left-hand side of (3.28a) to eliminate column $\hat{p}_{i-1}{}^{\nu+1}$. Note that in this progressive scheme as the index i varies across the shelf from $i = 2, \cdots, nz$ that the matrix α_{i-1}, and the vector $\hat{\beta}_{i-1}$ are known from the previous calculation at $i-1$. The α_i and $\hat{\beta}_i$ are calculated as

$$\alpha_i = -\frac{(a^+{}_i - s\,b^+{}_i - s^2c^+{}_i)}{(a^o{}_i - s\,b^o{}_i - s^2c^o{}_i) + (a^-{}_i - s\,b^-{}_i - s^2c^-{}_i)\alpha_{i-1}}; \tag{3.34a}$$

$$\hat{\beta}_i = \frac{(b^+{}_i + s\,c^+{}_i)\hat{p}_{i+1}{}^{\nu} + c^+{}_i\,\hat{q}_{i+1}{}^{\nu} + (b^o{}_i + s\,c^o{}_i)\hat{p}_i{}^{\nu} + c^o{}_i\,\hat{q}_i{}^{\nu}}{(a^o{}_i - s\,b^o{}_i - s^2c^o{}_i) + (a^-{}_i - s\,b^-{}_i - s^2c^-{}_i)\alpha_{i-1}} + \tag{3.34b}$$

$$\frac{(b^-{}_i + s\,c^-{}_i)\hat{p}_{i-1}{}^{\nu} + c^-{}_i\,\hat{q}_{i-1}{}^{\nu} - (a^-{}_i - s\,b^-{}_i - s^2c^-{}_i)\hat{\beta}_{i-1}}{(a^o{}_i - s\,b^o{}_i - s^2c^o{}_i) + (a^-{}_i - s\,b^-{}_i - s^2c^-{}_i)\alpha_{i-1}}.$$

When the column $i = nz$ is reached we need to solve for $\hat{p}_{nz}{}^{\nu+1}$. The column $\hat{p}_{nz+1}{}^{\nu+1}$ does not appear in the formulation of (3.28a) at the offshore boundary as the unknowns in that column were implicitly eliminated in (3.28a) by application of the offshore boundary condition. At $i = nz$ we have

$$(a^o{}_{nz} - s\,b^o{}_{nz} - s^2c^o{}_{nz})\hat{p}_{nz}{}^{\nu+1} + (a^-{}_{nz} - s\,b^-{}_{nz} - s^2c^-{}_{nz})\hat{p}_{nz-1}{}^{\nu+1} = \tag{3.35}$$

$$(b^o{}_{nz} + s\,c^o{}_{nz})\hat{p}_{nz}{}^{\nu} + c^o{}_{nz}\,\hat{q}_{nz}{}^{\nu} + (b^-{}_{nz} + s\,c^-{}_{nz})\hat{p}_{nz-1}{}^{\nu} + c^-{}_{nz}\,\hat{q}_{nz-1}{}^{\nu}.$$

From (3.29) there is also the relation

$$\hat{p}_{nz-1}{}^{\nu+1} = \alpha_{nz-1}\hat{p}_{nz}{}^{\nu+1} + \hat{\beta}_{nz-1}, \tag{3.36}$$

where α_{nz-1} and $\hat{\beta}_{nz-1}$ are already computed and available. The Equations (3.35) and (3.36) form a system of two equations in two unknowns namely $\hat{p}_{nz-1}{}^{\nu+1}$ and $\hat{p}_{nz}{}^{\nu+1}$. The system is conveniently solved by substituting (3.36) into (3.35) to eliminate $\hat{p}_{nz-1}{}^{\nu+1}$. The resulting equation for $\hat{p}_{nz}$ is

$$\hat{p}_{nz} = \frac{(b^{+}_{nz} + s\,c^{+}_{nz})\hat{p}_{nz+1}{}^{\nu} + c^{+}_{nz}\hat{q}_{nz+1}{}^{\nu}}{(a^{o}_{nz} - s\,b^{o}_{nz} - s^2c^{o}_{nz}) + (a^{-}_{nz} - s\,b^{-}_{nz} - s^2c^{-}_{nz})\alpha_{nz-1}} + \tag{3.37}$$

$$\frac{(b^{o}_{nz} + s\,c^{o}_{nz})\hat{p}^{-}_{nz}{}^{\nu} + c^{o}_{nz}\hat{q}_{nz}{}^{\nu} + (b^{-}_{nz} + s\,c^{-}_{nz})\hat{p}_{nz-1}{}^{\nu} + c^{-}_{nz}\hat{q}_{nz-1}}{(a^{o}_{nz} - s\,b^{o}_{nz} - s^2c^{o}_{nz}) + (a^{-}_{nz} - s\,b^{-}_{nz} - s^2c^{-}_{nz})\alpha_{nz-1}} -$$

$$\frac{(a^{-}_{nz} - s\,b^{-}_{nz} - s^2c^{-}_{nz})\hat{\beta}_{nz-1}}{(a^{o}_{nz} - s\,b^{o}_{nz} - s^2c^{o}_{nz}) + (a^{-}_{nz} - s\,b^{-}_{nz} - s^2c^{-}_{nz})\alpha_{nz-1}}.$$

With $\hat{p}_{nz}{}^{\nu+1}$ now known as well as all the α_i and $\hat{\beta}_i$ then immediately all the other $\hat{p}_i{}^{\nu+1}$ vectors in the domain are obtained using (3.29) as a recurrence relation. The solution for $\hat{q}_i{}^{\nu+1}$ is then readily determined by application of (3.28b).

3.5 Convergence Criteria

On each complete iteration through the domain a new pressure solution $\hat{P}^{\nu+1}$ is obtained from the solution $\hat{P}^{\nu}$ at the previous iteration. To initialize the procedure an arbitrary vector $\hat{P}^{o}$ is chosen. A convenient choice is to set all the elements of $\hat{P}^{o}$ to unity.

Convergence to a solution is detected using the Rayleigh Quotient which equals the present value of the shifted eigenvalue and is calculated as [Stewart, 1973]

$$\frac{1}{k - s} \doteq \frac{(\hat{P}^{\nu+1})^H \cdot \hat{P}^{\nu}}{(\hat{P}^{\nu+1})^H \cdot \hat{P}^{\nu+1}} \tag{3.38}$$

where the superscript H on vector $\hat{P}^{\nu+1}$ denotes the complex conjugate transpose. If the solution has converged then two successive iterations will produce values for the Rayleigh Quotient which differ by an amount less than some arbitrary small parameter ϵ. At convergence, the eigenvalue k is recovered from (3.38) since s is already known. The corresponding eigenvector is identified as $\hat{P}^{\nu+1}$.

CHAPTER FOUR

APPLICATION TO BAROCLINIC CTW's

In this Chapter the effect of a constant stratification on the propagation characteristics of CTW's shall be investigated. The propagation characteristics of CTW's are determined by a dispersion relation between their frequency and wavenumber. The main features of a CTW dispersion relation will be outlined by first presenting the simpler barotropic dispersion relation.

4.1 Barotropic Dispersion Relation

The shelf profile used to investigate the barotropic dispersion relations is the same as that studied by Buchwald and Adams [1968], namely

$$h = h_o e^{bx} \quad \text{for } 0 \leq x \leq L, \tag{4.1}$$
$$h = h_1 \quad \text{for } L < x \leq D.$$

The constants are chosen to be

$$h_o = 21.9 \text{ m},$$
$$b = 4.52 \times 10^{-5} \text{ m}^{-1},$$
$$L = 1.20 \times 10^5 \text{ m},$$
$$D = 1.60 \times 10^5 \text{ m},$$
$$h_1 = h_o e^{bL} = 4900 \text{ m}.$$

The Coriolis parameter is taken as $f = 1.0 \times 10^{-4} \text{ s}^{-1}$.

If the rigid lid approximation is made the CTW solutions for this shelf shape can be determined analytically [Buchwald and Adams, 1968]. For this solution the wavenumber k is the root of the transcendental equation

$$\tan(\alpha L) = \frac{-\alpha}{[\frac{b}{2} + k]}, \tag{4.2}$$

where the relation between α and k is given by

$$\alpha^2 + k^2 + \frac{b^2}{4} + \frac{bkf}{\omega} = 0. \tag{4.3}$$

At a given frequency ω, the analytical solutions obtained occur as a finite number of real wavenumber solutions and an infinite number of complex wavenumber solutions. The real solutions are the propagating modes and the complex solutions are the evanescent modes.

The distinction between real propagating and complex evanescent solutions is as follows. The wavenumber solution k will have a real component k_R and possibly a non zero imaginary component k_I such that

$$k = k_R + i\ k_I. \tag{4.4}$$

The wave solution has a harmonic alongshore dependence of the form e^{iky}. Substituting (4.4) into this dependence gives

$$e^{-k_I y} e^{ik_R y}. \tag{4.5}$$

The factor $e^{-k_I y}$ thus represents a growth or decay of the wave in the alongshore direction. A real propagating solution therefore has constant amplitude while a complex evanescent solution does not.

The barotropic dispersion curve for the real part of the wavenumber calculated analytically for the first three modes is presented in Figure 4.1 [Webster, 1985]. Frequency has been non-dimensionalized as $\sigma = \omega/f$ and the real part of the wavenumber as $\gamma_R = k_R/b$ where b is the shelf slope parameter.

The ratio of the frequency to the wavenumber at a given point on the dispersion curve gives the phase velocity as

$$C_p = -\frac{\omega}{k}, \tag{4.6}$$

which is the rate at which lines of constant phase propagate in the alongshore direction. The phase velocity may only be of negative (positive) sign in the northern (southern) hemisphere, hence CTW's only propagate with the coast on the right (left). The group velocity is the slope of the dispersion curve at a given wavenumber: that is

$$C_g = \frac{\partial \omega}{\partial k}. \tag{4.7}$$

The group velocity represents the velocity of energy propagation in the alongshore direction.

An important feature of the barotropic dispersion characteristics is that each propagating mode is frequency limited. That is, each mode has a subinertial frequency above which it may not exist as a propagating mode but must be evanescent. Below this cutoff frequency the propagating CTW's occur in modal pairs having the same mode number but having group velocities of opposite signs. The CTW in a modal pair is considered to be forward propagating if its group velocity is positive and to be backward propagating if its group velocity is negative.

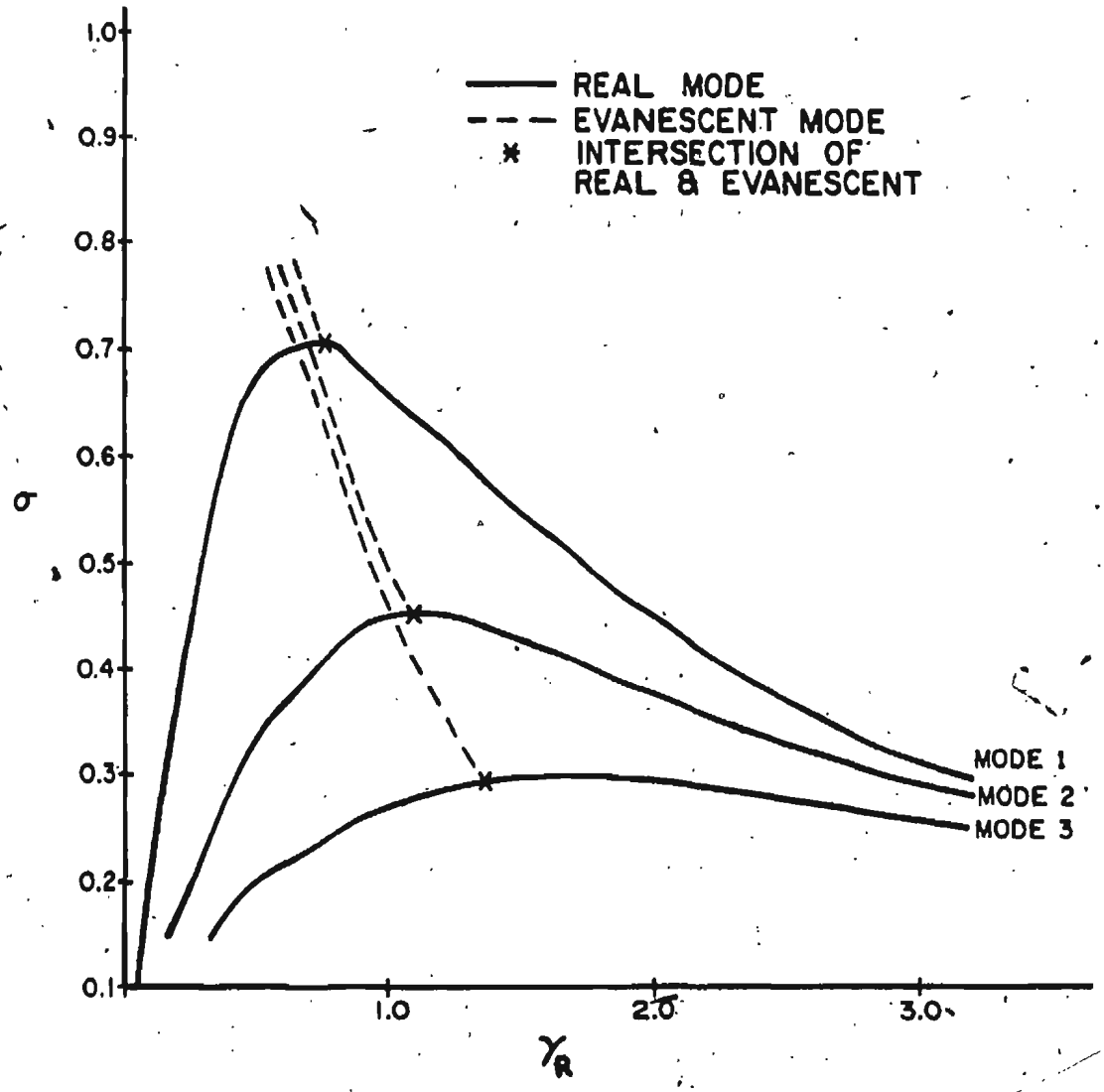

Figure 4.1 Dispersion diagram for the real part of the wavenumber for propagating and evanescent CTW modes for a barotropic ocean.

At the cutoff frequency the group velocity is zero. Above this frequency the evanescent modes split off from the propagating modes. The evanescent modes also occur as modal pairs. The members of an evanescent modal pair have wavenumbers that are complex conjugates of each other [Webster, 1985].

The baroclinic numerical scheme outlined in Chapter three is applied to the shelf profile (4.1) using an extremely small amount of stratification. The barotropic dispersion curve of Figure 4.1 is reproduced. The success of the numerical scheme in reproducing the analytical solution can be regarded as a partial verification of the scheme. A more complete verification is presented in Appendix C.

4.2 Baroclinic Dispersion Relation

The effects of density stratification on the dispersion characteristics are now investigated. The same shelf profile (4.1) is used with the same numerical parameters. A density stratification parameter is chosen [Chapman, 1983] such that

$$S = \frac{Nh_1}{fL}. \tag{4.8}$$

Note that the buoyancy frequency is defined in its usual dimensional form in the context of the stratification parameter. The stratification parameter is set to the values of $S = 0.2$ to simulate a weakly stratified ocean and $S = 1.0$ to simulate a strongly stratified ocean. The dispersion curves for both these cases are presented in Figures 4.2 and 4.3.

Stratification has the effect of increasing the phase speed of the forward propagating modes while decreasing the phase speed of the backward propagating modes [Chapman, 1983]. As well, at $S = 0.2$ a second zero of group velocity is introduced for each mode. As with the first zero of group velocity there are evanescent modes branching out from the second zero of group velocity. The second zero of group velocity differs from the first in that it defines the frequency below which a backwards propagating mode can not exist for the particular mode number. There exists a range of frequencies for a given mode through which that mode can exist as a long wave forward propagating mode, a short wave backward propagating mode, or an even shorter wave forward propagating mode.

Another feature of this particular choice of stratification parameter is the manner in which certain propagating modes are linked through the evanescent modes. For instance, there is an evanescent mode branching out from the second zero of group velocity of the first mode which eventually connects up to the first zero of group velocity of the third mode. As well, the evanescent mode branching out from the second zero of group velocity of the second mode connects to the first zero of group velocity of the fourth mode, although this is not depicted in Figure 4.2. The process of transformation of the mode two propagating mode into a mode four propagating mode will be presented in the next section.

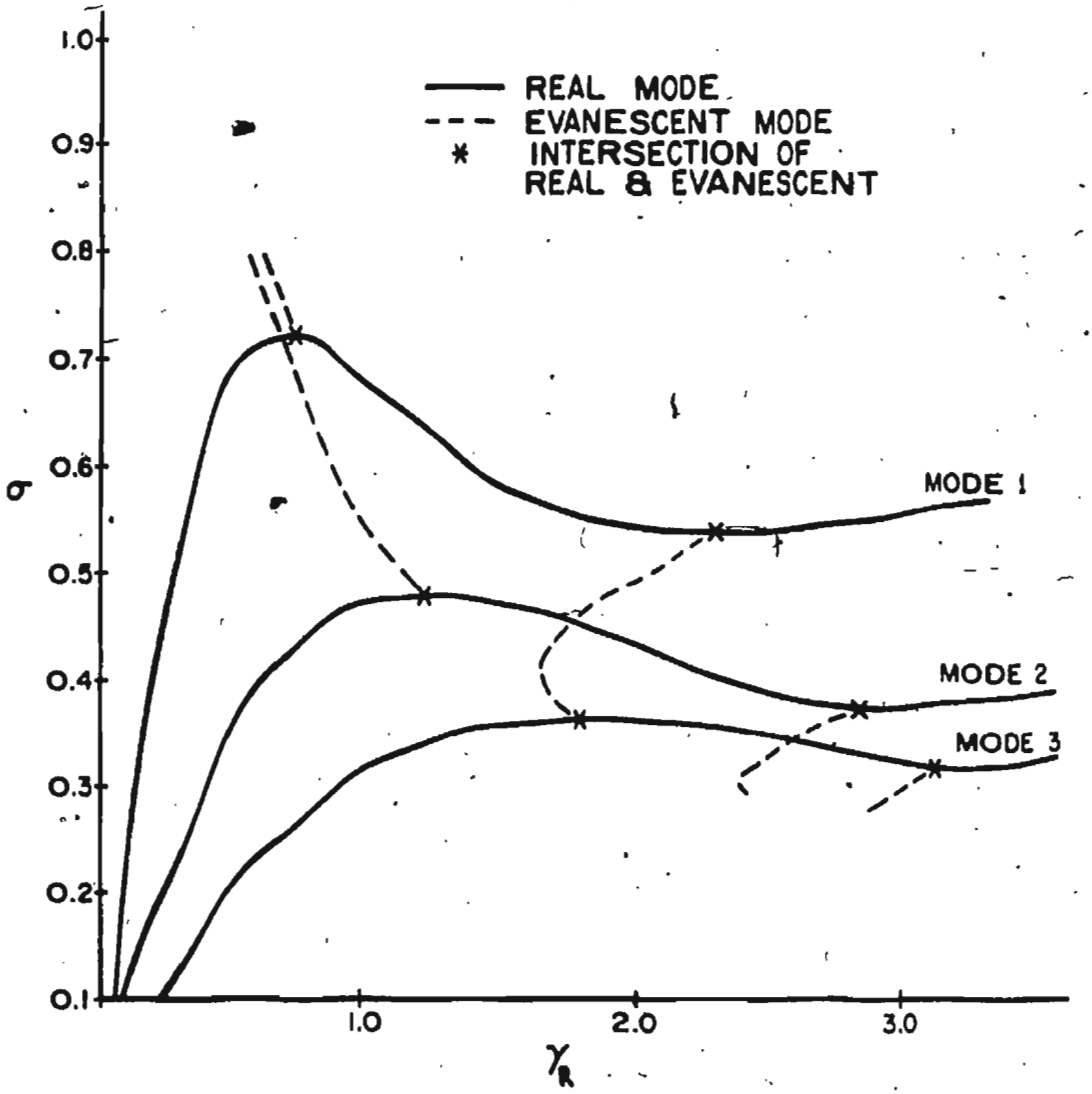

Figure 4.2 Dispersion diagram for the real part of the wavenumber for propagating and evanescent CTW modes for a baroclinic ocean; S = 0.2.

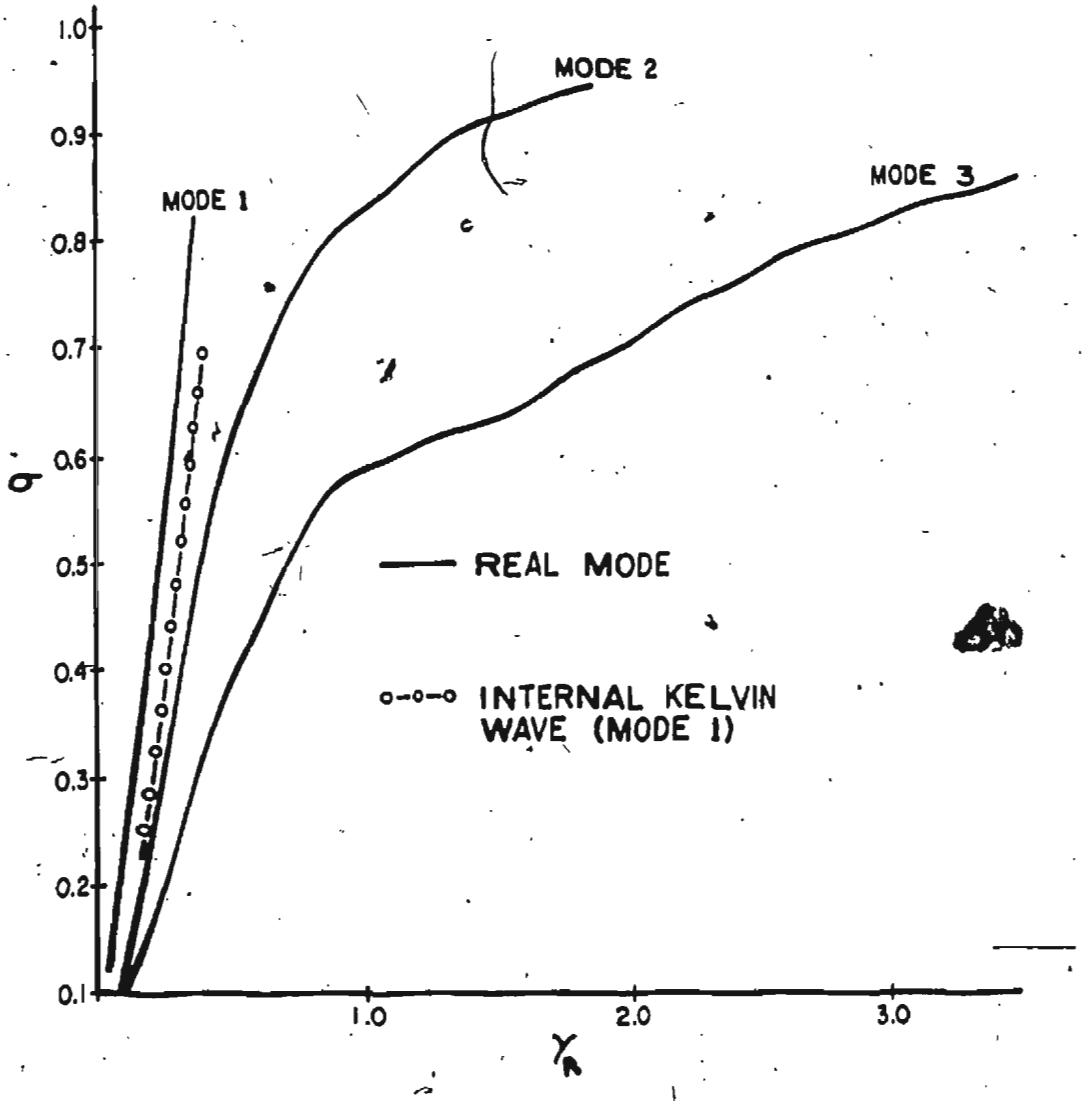

Figure 4.3 Dispersion diagram for the real part of the wave-number for propagating and evanescent CTW modes for a baroclinic ocean; S = 1.0.

For the strongly stratified case ($S = 1.0$), all three propagating modes are no longer frequency limited. These modes exist right up to the inertial frequency. Neither propagating mode has a zero of group velocity and consequently there are no evanescent modes splitting off from the propagating modes. The dispersion curves suggest that the waves are tending towards a non-dispersive Kelvin wave nature. This premise is supported by analytically computing the baroclinic Kelvin wave dispersion relation (see Appendix D) for a flat bottom ocean of depth $h_1 = 4000$ m. For the first mode baroclinic Kelvin wave the dispersion curve lies close to the mode one CTW dispersion curve for $S = 1.0$ (see Figure 4.3). The stratification parameter may be interpreted as the ratio of the baroclinic radius of deformation NH/f to the offshore length scale L. It is expected that as S is increased and hence the baroclinic radius is increased that the CTW's will begin to see the coast as a vertical wall. In the limit of large stratification the CTW dispersion relation would therefore approach the baroclinic Kelvin wave dispersion relation [Chapman, 1983].

4.3 Fixed Frequency

Figure 4.4 shows the locations of the non-dimensionalized wavenumber solutions in the complex plane for the lowest five modes at a fixed frequency of $\sigma = 0.3$ for variable stratification. Note again that the non-dimensionalized wavenumber is defined as $\gamma = k/b$ which has a real component $\gamma_R = k_R/b$ and

imaginary component $\gamma_I = k_I/b$. The stratification parameter is varied from $S = 0.01$ to $S = 0.4$.

The wavenumbers of the forward propagating modes one (1F), two (2F), and three (3F) decrease as S is increased. This behavior is consistent with the results of the previous section. The wavenumbers of the evanescent modes four (4E) and five (5E) apparently remain complex as S is increased to 0.4. For the backward propagating modes one (1B), two (2B), and three (3B), increasing S first results in the wavenumber increasing along the real axis. At an intermediate value of S for each mode a second forward propagating mode one (1F'), two (2F'), and three (3F') appears along the real axis. At a slightly higher stratification for each mode the backward and the second forward propagating mode coalesce. At this point γ leaves the real axis and does a reverse loop in the complex plane. The evanescent modes occur as complex conjugates of each other. This is evident by taking the complex conjugate of (3.18). Since $\mathbf{M}$ is purely real then $\mathbf{M} = \mathbf{M}'$ where $'$ is used to denote the complex conjugate. Consequently, if λ and ξ are solutions of (3.18) then λ' and ξ' are also solutions. Since the complex γ occur as conjugate solutions, the joining of the two real solutions produces two complex solutions. The mode two dispersion curve eventually rejoins the real axis and splits into a mode four forward and backward propagating mode. Thus, it appears that a process by which a given mode may transform into another mode, has been established.

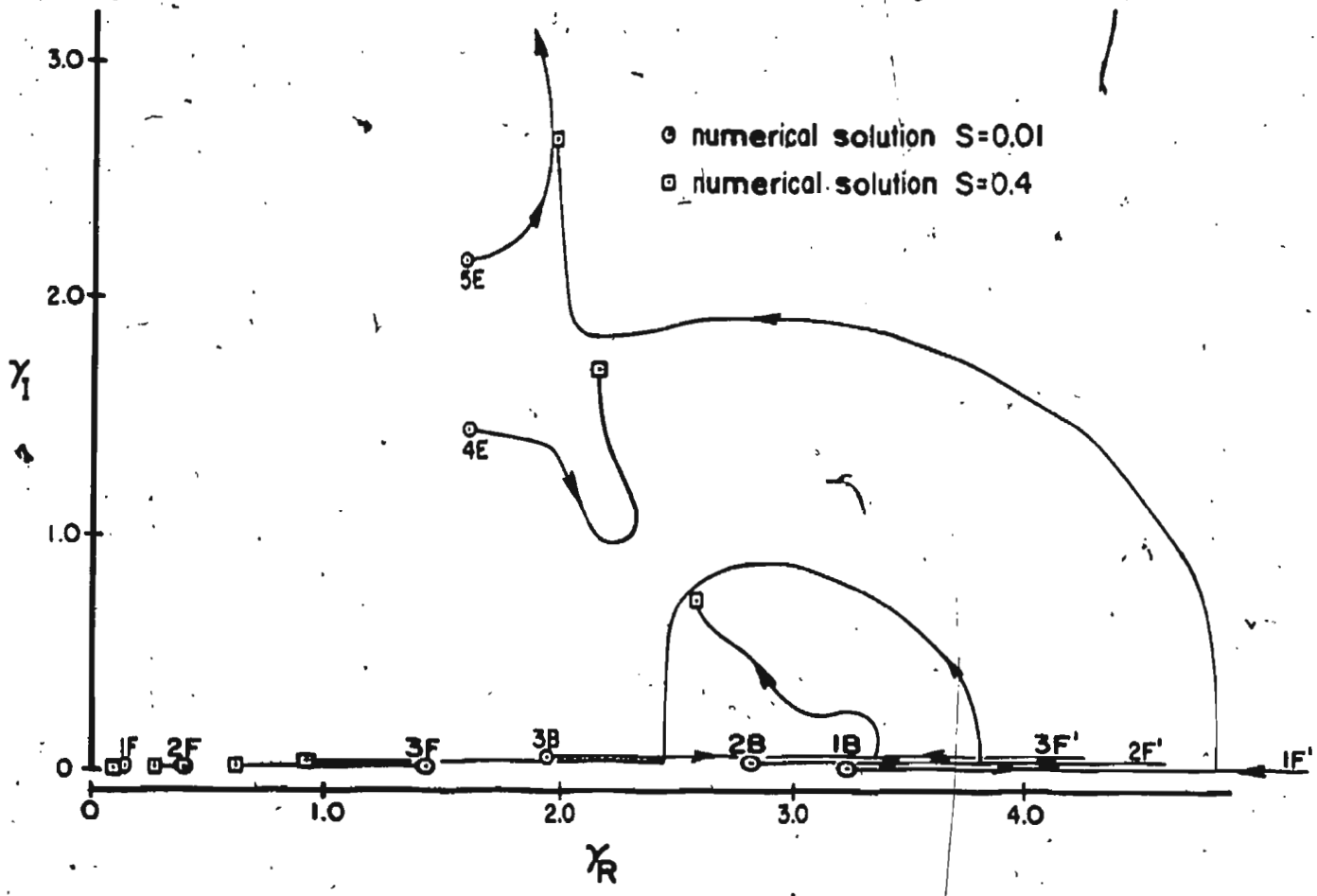

Figure 4.4 Loci of wavenumber solutions on the complex plane for $\sigma = 0.3$ and for S varied between 0.01 and 0.4. The mode numbers are indicated. F designates a forward propagating mode, B a backward propagating mode, and E an evanescent mode.

4.4 Rate of Convergence

This Chapter is concluded by presenting a note concerning the manner in which a dispersion curve is produced. The numerical scheme outlined in Chapter three is implemented as a Fortran 77 program on a VAX 11/785 computer using double precision complex arithmetic (14 digit accuracy).

To obtain results from the model it is necessary to specify: horizontal nx and vertical nz grid spacing, the bottom topography $h(x)$, the shelf length L, the extent of the grid in the offshore direction D, the Coriolis parameter f, the wave frequency ω, an estimate of the wavenumber s, and an arbitrary initial vector ξ^o. The program will then seek a wavenumber solution k which is close to s. If the solution converges then a dispersion pair (ω,k) is identified. If the solution does not converge within a specified number of iterations then execution is terminated.

The solution may fail for any one of several reasons. First, if there is no wavenumber solution k in the vicinity of the shift s then convergence will not occur quickly enough. Secondly, certain choices of input parameters may lead to extremely large matrix coefficients. As the computer can not handle such numbers the solution fails. Thirdly, convergence to a complex solution can never be obtained with a real shift as complex conjugate solutions occur in conjugate pairs both of which are the exact same distance from any real shift.

The generation of the curves in Figures 4.1 through 4.4 requires the computation of a large number of such wavenumber solutions. Once an (ω,k) pair for any curve has been identified then the rate of convergence for all successive solu-

tions on that curve may be improved by a factor of five. This is achieved by using the eigenvector of the previous solution as the initial vector ξ^o of the present solution. As well, the choice of shift s may be optimized by choosing it to lie along a linear extrapolation of a portion of the curve already determined.

CHAPTER FIVE

INCLUSION OF A BAROCLINIC SHEAR CURRENT

In this Chapter, the previous model is extended to include a baroclinic shear current flowing parallel to the coast to determine how the phase speeds of CTW's are influenced. Results are obtained for comparison with observations of CTW propagation made during the Australian Coastal Experiment [Freeland *et al.*, 1986].

5.1 Equations

The mean states of density, pressure, and velocity are designated by ρ_o, p_o, and $\vec{U}_o$ respectively. The total density field ρ, pressure field p, and velocity field $\vec{U}$ are composed of the mean fields and the perturbation fields ρ', p', and $\vec{U}'$ due to the presence of wave motion so that

$$\rho = \rho_o(x,z) + \rho'(x,y,z,t), \tag{5.1a}$$

$$p = p_o(x,z) + p'(x,y,z,t), \tag{5.1b}$$

$$\vec{U} = \vec{U}_o(x,z) + \vec{U}'(x,y,z,t). \tag{5.1c}$$

The mean current has only one component parallel to the coastline denoted by v_o.

The perturbation equations are derived from the mass conservation, the continuity, and the momentum equations in a manner analogous to that of Chapter two. The differential form of the density equation is Equation (2.11). After utilizing (5.1a) and (5.1c) for the density and velocity fields, it becomes

$$\frac{\partial \rho'}{\partial t} + u'\frac{\partial \rho_o}{\partial x} + u'\frac{\partial \rho'}{\partial x} + v_o\frac{\partial \rho'}{\partial y} + v'\frac{\partial \rho'}{\partial y} + w'\frac{\partial \rho_o}{\partial z} + w'\frac{\partial \rho'}{\partial z} = 0. \qquad (5.2)$$

Assuming that the perturbation quantities are much smaller than the corresponding mean state quantities then this equation can be linearized to

$$\frac{\partial \rho'}{\partial t} + u'\frac{\partial \rho_o}{\partial x} + v_o\frac{\partial \rho'}{\partial y} + w'\frac{\partial \rho_o}{\partial z} = 0. \qquad (5.3)$$

The continuity Equation (2.9) remains as is because v_o has no y dependence. Hence,

$$\frac{\partial u'}{\partial x} + \frac{\partial v'}{\partial y} + \frac{\partial w'}{\partial z} = 0. \qquad (5.4)$$

For the momentum equations the time-dependent flow is separated from the mean flow. Substituting the relations (5.1) into the momentum Equations (2.1) gives the three component equations

$$\frac{\partial u'}{\partial t} + u'\frac{\partial u'}{\partial x} + (v_o + v')\frac{\partial u'}{\partial y} + w'\frac{\partial u'}{\partial z} - f(v_o + v') = \qquad (5.5a)$$

$$\frac{-1}{\rho_o}\frac{\partial (p_o + p')}{\partial x},$$

$$\frac{\partial (v_o + v')}{\partial t} + u'\frac{\partial (v_o + v')}{\partial x} + (v_o + v')\frac{\partial v'}{\partial y} + w'\frac{\partial (v_o + v')}{\partial z} + fu' = \qquad (5.5b)$$

$$-\frac{1}{\rho_o}\frac{\partial p'}{\partial y},$$

$$\frac{\partial w'}{\partial t} + u'\frac{\partial w'}{\partial x} + (v_o + v')\frac{\partial w'}{\partial y} + w'\frac{\partial w'}{\partial z} = \tag{5.5c}$$

$$-\frac{1}{(\rho_o + \rho')}\frac{\partial(p_o + p')}{\partial z} - g,$$

where the Boussinesq approximation has been adopted. Linearizing and time averaging these equations produces from (5.5a) the geostrophic relation

$$f v_o = \frac{1}{\rho_o}\frac{\partial p_o}{\partial x}, \tag{5.6a}$$

and from (5.5c) the hydrostatic relation

$$-\rho_o g = \frac{\partial p_o}{\partial z}. \tag{5.6b}$$

Subtracting the mean state Equations (5.6) from the Equations (5.5) and linearizing the resulting equations gives the perturbation equations as

$$\frac{\partial u'}{\partial t} + v_o\frac{\partial u'}{\partial y} - f v' = -\frac{1}{\rho_o}\frac{\partial p'}{\partial x}, \tag{5.7}$$

$$\frac{\partial v'}{\partial t} + u'\frac{\partial v_o}{\partial x} + v_o\frac{\partial v'}{\partial y} + w'\frac{\partial v_o}{\partial z} + f u' = -\frac{1}{\rho_o}\frac{\partial p'}{\partial y}, \tag{5.8}$$

$$-\rho' g = \frac{\partial p'}{\partial z}. \tag{5.9}$$

The five perturbation Equations (5.3), (5.4), (5.7), (5.8), and (5.9) in the five unknowns p', ρ', u', v', and w' may be solved explicitly for the perturbation pressure p'.

5.2 Long-Wave Approximation

Analogous to the treatment presented in Chapter two, the perturbation equations may be formulated as a generalized discrete eigenvalue problem in pressure. It turns out that the resulting equation is of fifth power in the eigenvalue k. The equation is of the form

$$\mathbf{A}\hat{P} = k\mathbf{B}\hat{P} + k^2\mathbf{C}\hat{P} + k^3\mathbf{D}\hat{P} + k^4\mathbf{E}\hat{P} + k^5\mathbf{F}\hat{P}. \tag{5.10a}$$

The methods outlined earlier may be employed to solve such an equation resulting in an expanded dimensional space equal to five times the original space. Making the long wave approximation reduces this problem to a linear eigenvalue problem as

$$\mathbf{A}\hat{P} = k\mathbf{B}\hat{P}. \tag{5.10b}$$

Another consequence is that the waves become nondispersive in the long-wavelength limit. Making the approximation in effect means that the offshore momentum Equation (5.7) is a purely geostrophic balance between perturbation velocity v' and the cross shelf perturbation pressure gradient $\frac{\partial p'}{\partial z}$ as

$$fv' = \frac{1}{\rho_o}\frac{\partial p'}{\partial z}. \tag{5.11}$$

For the approximation to be valid we assume the conditions $kL \ll 1$, $kv_o \ll f$, and and $\omega \ll f$ to be satisfied. Applying a scaling argument to (5.4) and use of the condition $kL \ll 1$ indicates that the offshore velocity u' is smaller than the alongshore velocity v' by a factor of order kL [Gill and

Schumann, 1974]. The term $\frac{\partial u'}{\partial t}$ may be neglected in (5.7) in comparison with fv' as the neglected term is smaller than fu' by the product of the two terms kl and $\frac{\omega}{f}$. As well, the term $v_o \frac{\partial u'}{\partial y}$ may be neglected in comparison with fv'. This time the neglected term is smaller than fv' by the product of the two terms kL and $\frac{kv_o}{f}$. Taking a maximum allowable alongshore velocity v_o to be of order 1 ms^{-1}, k of order 10^{-6} m^{-1}, L of order 10^5 m, and f of order 10^{-5} s^{-1}, then the terms kL and kv_o are both of order 0.1. Their product is then of order 0.01. Also note that since the geostrophic assumption is made in only one coordinate direction the equations used are termed semi-geostrophic.

5.3 Pressure Formulation

As in Chapter two, solutions are sought which have the harmonic time and alongshore dependencies $e^{i(ky + \omega t)}$ where k is the alongshore wavenumber and ω is the frequency. The equations of motion are reduced from a four-dimensional problem in x, y, z, and t to a two-dimensional one in x and z. Each of the five perturbation quantities is now denoted by double prime superscripts in accordance with (2.13). The equations are

$$i\omega\rho'' + u''\frac{\partial \rho_o}{\partial z} + ikv_o\rho'' + w''\frac{\partial \rho_o}{\partial z} = 0, \tag{5.12a}$$

$$\frac{\partial u''}{\partial z} + ikv'' + \frac{\partial w''}{\partial z} = 0, \tag{5.12b}$$

$$fv'' = \frac{1}{\rho_o}\frac{\partial p''}{\partial z}, \tag{5.12c}$$

$$i\omega v'' + u''\frac{\partial v_o}{\partial z} + ikv_o v'' + w''\frac{\partial v_o}{\partial z} + fu'' = \frac{-ikp''}{\rho_o}, \tag{5.12d}$$

$$\rho''g = \frac{\partial p''}{\partial z}. \tag{5.12e}$$

The Equations (5.12a), (5.12c), (5.12d), and (5.12e) are solved for the three perturbation velocity components as

$$u'' = k\,f_5\frac{\partial p''}{\partial z} + f_4\frac{\partial p''}{\partial z} + k\,f_3\frac{\partial p''}{\partial z} + f_2\frac{\partial p''}{\partial z} + k\,f_1 p'', \tag{5.13a}$$

$$v'' = f_{11}\frac{\partial p''}{\partial z}, \tag{5.13b}$$

$$w'' = k\,f_{10}\frac{\partial p''}{\partial z} + f_9\frac{\partial p''}{\partial z} + k\,f_8\frac{\partial p''}{\partial z} + f_7\frac{\partial p''}{\partial z} + k\,f_6 p'', \tag{5.13c}$$

where the functions prefixed by f are introduced for convenience reasons as

$$f_0 = \frac{\partial \rho_o}{\partial z}\frac{\partial v_o}{\partial z} - \frac{\partial \rho_o}{\partial z}\frac{\partial v_o}{\partial z} - f\frac{\partial \rho_o}{\partial z}, \tag{5.14a}$$

$$f_1 = \frac{\dfrac{\partial \rho_o}{\partial z}}{\rho_o f_0}, \tag{5.14b}$$

$$f_2 = \frac{\omega\dfrac{\partial \rho_o}{\partial z}}{f\,\rho_o f_0}, \tag{5.14c}$$

$$f_3 = \frac{v_o \frac{\partial \rho_o}{\partial z}}{f \rho_o f_0}, \tag{5.14d}$$

$$f_4 = \frac{\omega \frac{\partial v_o}{\partial z}}{g f_0}, \tag{5.14e}$$

$$f_5 = \frac{v_o \frac{\partial v_o}{\partial z}}{g f_0}, \tag{5.14f}$$

$$f_6 = -\frac{\frac{\partial \rho_o}{\partial x}}{\rho_o f_0}, \tag{5.14g}$$

$$f_7 = -\frac{\omega \frac{\partial \rho_o}{\partial x}}{f \rho_o f_0}, \tag{5.14h}$$

$$f_8 = -\frac{v_o \frac{\partial \rho_o}{\partial z}}{f \rho_o f_0}, \tag{5.14i}$$

$$f_9 = -\frac{(\omega \frac{\partial v_o}{\partial z} + \omega f)}{g f_0}, \tag{5.14j}$$

$$f_{10} = -\frac{(v_o \frac{\partial v_o}{\partial x} + v_o f)}{g f_0}, \tag{5.14k}$$

$$f_{11} = \frac{1}{f \rho_o}. \tag{5.14l}$$

The equation for pressure in the interior is obtained by substituting the expressions (5.13) for velocities into the continuity Equation (5.12b). The interior

equation becomes

$$f_9\frac{\partial^2 p''}{\partial z^2} + (\frac{\partial f_9}{\partial z} + \frac{\partial f_4}{\partial x})\frac{\partial p''}{\partial z} + f_2\frac{\partial^2 p''}{\partial x^2} + (\frac{\partial f_7}{\partial z} + \frac{\partial f_2}{\partial x})\frac{\partial p''}{\partial x} + \tag{5.15}$$

$$(f_7 + f_4)\frac{\partial^2 p''}{\partial x z} = -k\Big[f_{10}\frac{\partial^2 p''}{\partial x^2} + (f_6 + \frac{\partial f_5}{\partial x} + \frac{\partial f_{10}}{\partial z})\frac{\partial p''}{\partial z} +$$

$$(f_8 + f_5)\frac{\partial^2 p''}{\partial x z} + (\frac{\partial f_8}{\partial z} + \frac{\partial f_3}{\partial x} + f_{11} + f_1)\frac{\partial p''}{\partial x} + (\frac{\partial f_6}{\partial z} + \frac{\partial f_1}{\partial x})p''\Big].$$

The pressure equations along the boundaries are determined from considering the behavior of the velocities there. Along the vertical coastal wall we have

$$u'' = 0, \tag{5.16a}$$

so

$$f_4\frac{\partial p''}{\partial z} + f_2\frac{\partial p''}{\partial x} = -k\Big[f_5\frac{\partial p''}{\partial z} + f_3\frac{\partial p''}{\partial x} + f_1 p''\Big]. \tag{5.16b}$$

Along the surface and the flat bottom

$$w'' = 0, \tag{5.17a}$$

so

$$f_9\frac{\partial p''}{\partial z} + f_7\frac{\partial p''}{\partial x} = -k\Big[f_{10}\frac{\partial p''}{\partial z} + f_8\frac{\partial p''}{\partial x} + f_6 p''\Big]. \tag{5.17b}$$

On the sloping shelf bottom

$$u''\frac{\partial h}{\partial x} + w'' = 0, \tag{5.18a}$$

so

$$(f_4\frac{\partial h}{\partial x} + f_9)\frac{\partial p''}{\partial z} + (f_2\frac{\partial h}{\partial x} + f_7)\frac{\partial p''}{\partial x} = \tag{5.18b}$$

$$-k\left[(f_5\frac{\partial h}{\partial x} + f_{10})\frac{\partial p''}{\partial z} + (f_3\frac{\partial h}{\partial x} + f_8)\frac{\partial p''}{\partial x} + (f_1\frac{\partial h}{\partial x} + f_6)p''\right].$$

At the offshore boundary

$$\frac{\partial u''}{\partial x} = 0, \tag{5.19a}$$

so

$$\frac{\partial f_4}{\partial x}\frac{\partial p'}{\partial z} + f_2\frac{\partial^2 p''}{\partial x^2} + f_4\frac{\partial^2 p''}{\partial x z} + \frac{\partial f_2}{\partial x}\frac{\partial p''}{\partial x} = \tag{5.19b}$$

$$-k\left[f_5\frac{\partial p''}{\partial z} + f_3\frac{\partial^2 p''}{\partial x^2} + f_5\frac{\partial^2 p''}{\partial x z} + (\frac{\partial f_3}{\partial x} + f_1)\frac{\partial p''}{\partial x} + \frac{\partial f_1}{\partial x}p''\right].$$

To solve the equations for pressure they are first transformed from the irregular shelf geometry into a rectangular domain by the same vertically stretched coordinate transformation as utilized in Chapter two. In transformed space the derivatives are approximated by centered finite difference expressions. From the resulting equations the problem is formulated as a matrix eigenvalue problem in which the elements of the matrix are derived from the coefficients of the equations. Even with the equations in the semi-geostrophic form the [redacted] of the terms that form the matrix elements is formidable. The entire procedure involves a long series of algebraic manipulations and consequently it is carried out using a computer program called Macsyma which is an algebraic symbolic manipulator [Bogen, 1983]. It is capable of generating the necessary computer code to set-up and define all the elements of the required matrices.

5.4 Mean Velocity and Density Fields

To solve the problem it is necessary to specify the mean velocity field $v_o(x,z)$, the mean density field $\rho_o(x,z)$, and their derivatives. However, the mean velocity and density fields are related through the geostrophic (5.6a) and hydrostatic (5.6b) equations. In the following development, the mean velocity field will be used to determine the mean density field.

Starting from the geostrophic equation for the mean flow, differentiating with respect to z, interchanging the order of differentiation for p_o, using the hydrostatic relation, assuming f to be constant, and using ρ_o in the Boussinesq sense gives the thermal wind equation

$$f\frac{\partial v_o}{\partial z} = -\frac{g}{\rho_o}\frac{\partial \rho_o}{\partial x}. \tag{5.20}$$

Equation (5.20) states that the horizontal gradient of density is

$$\frac{\partial \rho_o}{\partial x} = -\frac{f\,\rho_o}{g}\frac{\partial v_o}{\partial z}. \tag{5.21}$$

If the buoyancy frequency is specified over an entire vertical column, say at the furthest offshore column of the discrete domain, then the vertical gradient of density $\frac{\partial \rho_o}{\partial z}$ is known all along that column. That is, from the definition of buoyancy frequency

$$\frac{\partial \rho_o}{\partial z} = -\frac{\rho_o}{g}N^2(z). \tag{5.22}$$

The actual density field $\rho_o(x,z)$ itself is computed by first integrating in the z direction from $(D,0)$ to a depth z at (D,z) as

$$\rho_o(D,z) = \rho_o(D,0) + \int_0^z \frac{\partial \rho_o}{\partial z} dz \,, \tag{5.23a}$$

where the valde of ρ_o at the point $(D,0)$ is chosen to be $\rho_o(D,0) = 1035.0$ kg m^{-3} and the z gradient is known from (5.22). The integration is then carried out in the x direction from (D,z) to (x,z)

$$\rho_o(x,z) = \rho_o(D,z) + \int_D^x \frac{\partial \rho_o}{\partial x} dx \,, \tag{5.23b}$$

where the x gradient is known from (5.21). This procedure is carried out for each point on the x, z grid.

5.5 Application

An experimental program was carried out along the eastern coast of Australia to investigate the existence of CTW's [Freeland *et al.*, 1986]. Observational evidence suggested the presence of the first three forward propagating modes. The theoretical phase speed of each of theses modes was computed, at a frequency of 10 percent of the Coriolis frequency, using a numerical model [Brink and Chapman, 1985]. The model allowed for realistic topography and stratification. The experimental determination of phase speeds was computed using two different data analysis techniques. First, Freeland *et al.* performed a modal decomposition in the frequency domain. The experimental phase speeds

systematically exceeded the theoretical phase speeds by about 25 percent for all three modes. Secondly, Church *et al.* [1986] performed a modal decomposition in the time domain. Using this method, the experimental phase speeds did not exceed the theoretical values. Moreover, the phase speeds were closer to the theoretical values than those of Freeland *et al.* The mode one CTW was about 20 percent slower; the mode two about 10 percent slower. In either case the theory and experiment were unable to produce congruent results.

In the Australian experiment a mean current was measured to flow in the direction opposite to the direction of phase propagation of the CTW's. Using the model developed in this Chapter, theoretical values for the phase speeds of CTW's in the presence of a mean baroclinic alongshore current are to be computed. These revised theoretical values shall be compared to the experimental values.

An offshore topography, a vertical stratification profile, and a mean velocity profile are chosen from data kindly supplied by H.J. Freeland. The data chosen is representative of the offshore line at Newcastle. The shelf topography is fitted to an exponential profile using a least squares fit (see Figure 5.1). The profile is Equation (4.1) with $h_o = 29.2$ m, $h_1 = 4800.0$ m, $b = 5.10\times10^{-5}$ m^{-1}, $L = 100.0$ km, $D = 120.0$ km. The vertical stratification profile at $z = D$ is modeled by

$$N^2(z) = N_o^2 e^{-\alpha z} + N_c^2, \tag{5.24}$$

where N_o is the maximum value of the buoyancy frequency at the surface, α is the vertical decay scale of the buoyancy frequency, and N_c is a constant

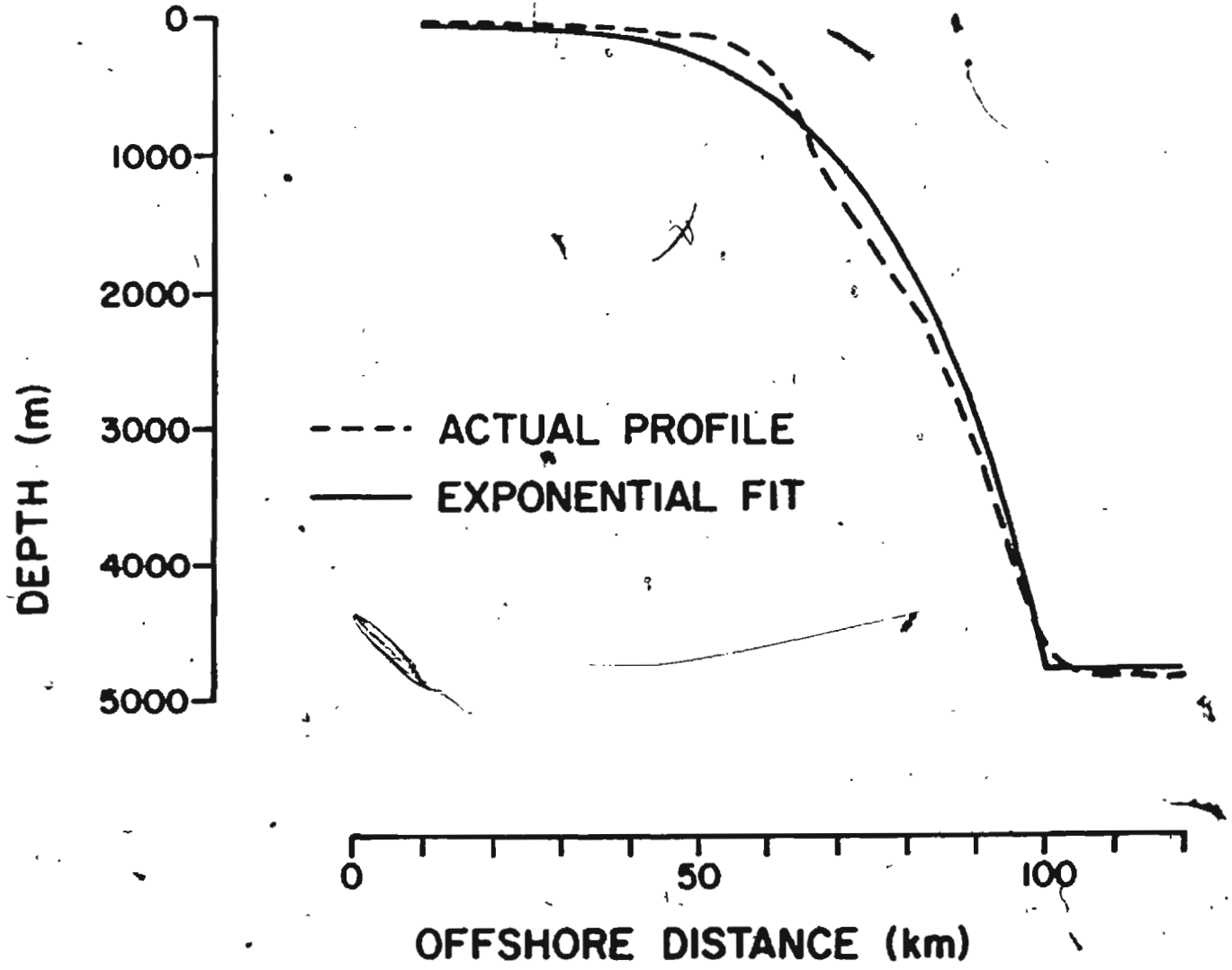

Figure 5.1 Comparison of actual shelf profile at the Newcastle line with the fitted exponential shelf.

stratification of small numerical value. The parameter N_c is required because the decay of stratification is so rapid that the ocean is effectively barotropic near the bottom. It is necessary to have some stratification there to prevent the computer program from failing due to numerical reasons. The parameters appropriate to the coast of Australia are $N_0^2 = 3.0\times10^{-4}\ s^{-2}$, $\alpha = 0.142\ km^{-1}$, and $N_c^2 = 1.0\times10^{-10}\ s^{-2}$.

Originally, the mean velocity field was determined from current meter data for the Australian experiment by tailoring the data to the requirements of the numerical scheme using a bi-cubic spline to interpolate velocity values at all grid points. However, with the sparse data available it was difficult to carry out the interpolation over the entire domain. Instead an analytical expression which approximately modeled features of the behavior of the observed mean velocity field was chosen. The choice of an analytical expression for the mean velocity field immediately allows easy computation of velocity gradients as well as density field and density gradients.

The mean shear current is modeled as a coastal jet. In the horizontal direction the velocity profile is taken to behave as a Gaussian function which is characterized by a maximum amplitude a, its centre position x_c, and its width b over the shelf. The vertical dependence is modeled as an exponentially decaying function with a vertical decay scale of c. The combination of these functional dependencies results in the type of shear current in Figure 5.2 where the center of the current has been positioned over the shelf break. The analytical expression for the shear current is

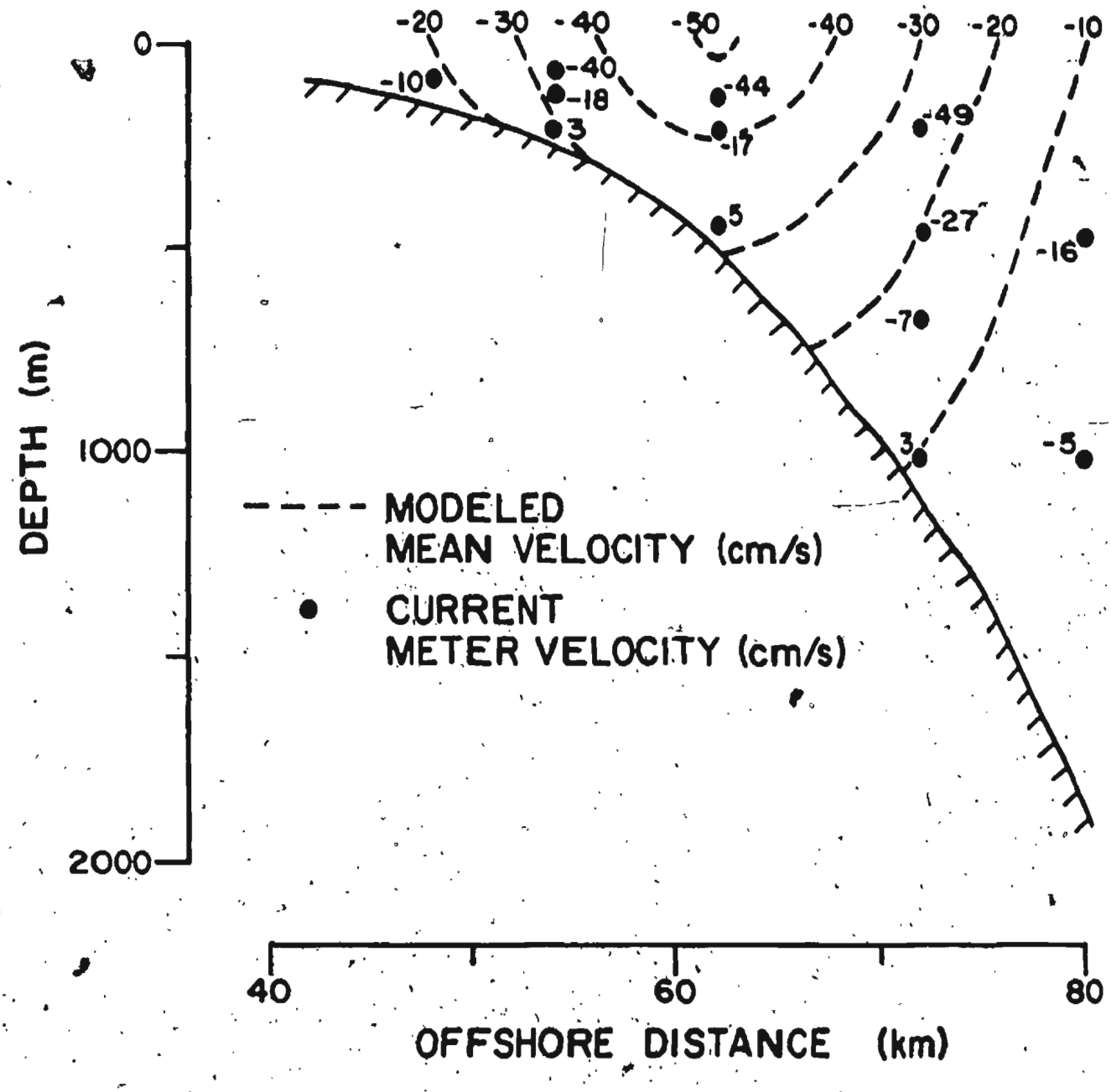

Figure 5.2 Comparison of current meter measurements with modeled mean alongshore current.

$$v_o(z,z) = ae^{-\frac{(z-z_c)^2}{2b^2}} e^{cz} \tag{5.25}$$

The parameters appropriate to the coast of Australia are $a = -50$ cm s^{-1}, $b = 10$ km, $c = 0.001$ m^{-1}, and $z_c = 60$ km.

Also depicted in Figure 5.2 are the current meter measurements at various locations. Clearly, the agreement between modeled current and current measurements is rough. However, the modeled current does at least reflect the vertical decay of current with depth as well as the decrease in current towards both the deep sea and the coast.

The associated density field was calculated using (5.23) as

$$\rho_o(z,z) = \rho_o(D,0) + \rho_o(D,0)\frac{N_o^2 e^{az} + \alpha N_c^2 z - N_o^2}{\alpha g} + \tag{5.26}$$

$$acf\ \rho_o(D,0)\frac{\sqrt{2\pi}b\left(erf\left(\frac{\sqrt{2}D - \sqrt{2}z_c}{2b}\right)e^{cz} + erf\left(\frac{\sqrt{2}z_c - \sqrt{2}z}{2b}\right)e^{cz}\right)}{2g}.$$

5.6 Results

By varying a in (5.25) it is possible to observe the effect of varying the strength of the shear current on the wavenumber of a given mode. The effect of a baroclinic shear current on the wavenumbers of modes one, two, and three is illustrated in Figures 5.3, 5.4, and 5.5 respectively. Note that positive (negative) velocities correspond to a shear current flowing in the same (opposite) direction as the phase propagation of the wave.

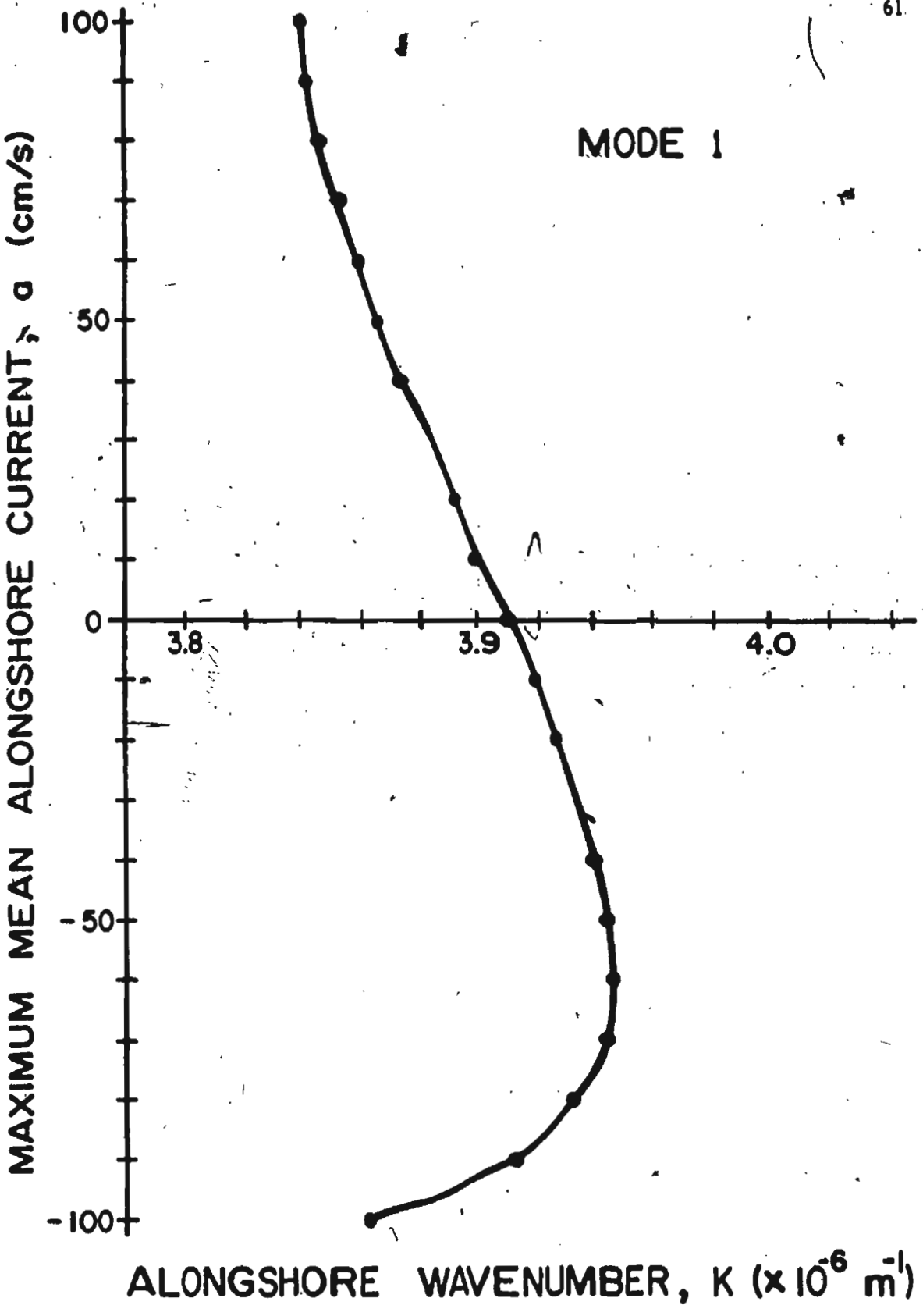

Figure 5.3 Behavior of alongshore wavenumber k for mode one CTW for varying strength and direction of mean alongshore current. Non-dimensional frequency equal to 0.1.

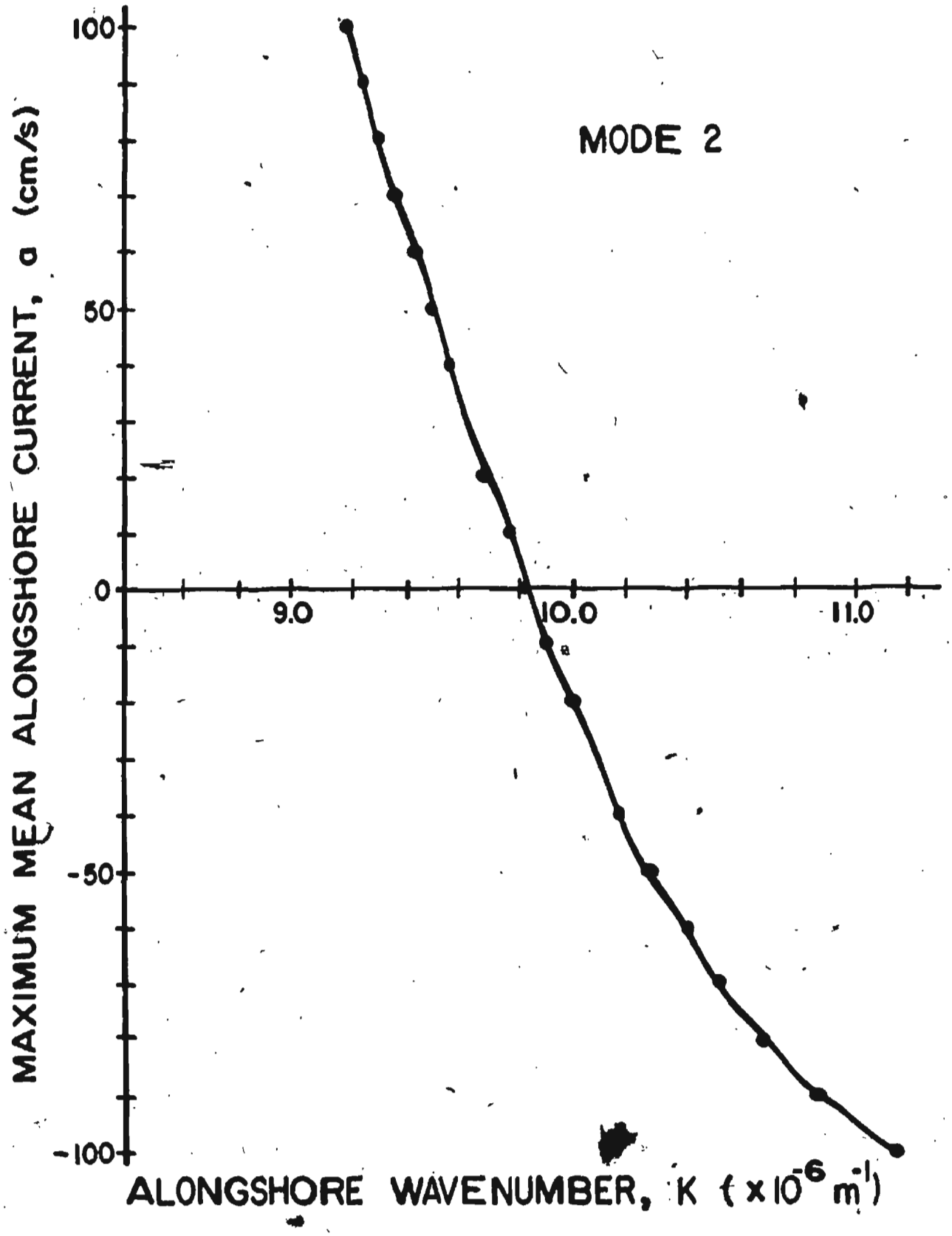

Figure 5.4 Behavior of alongshore wavenumber k for mode two CTW for varying strength and direction of mean alongshore current. Non-dimensional frequency equal to 0.1.

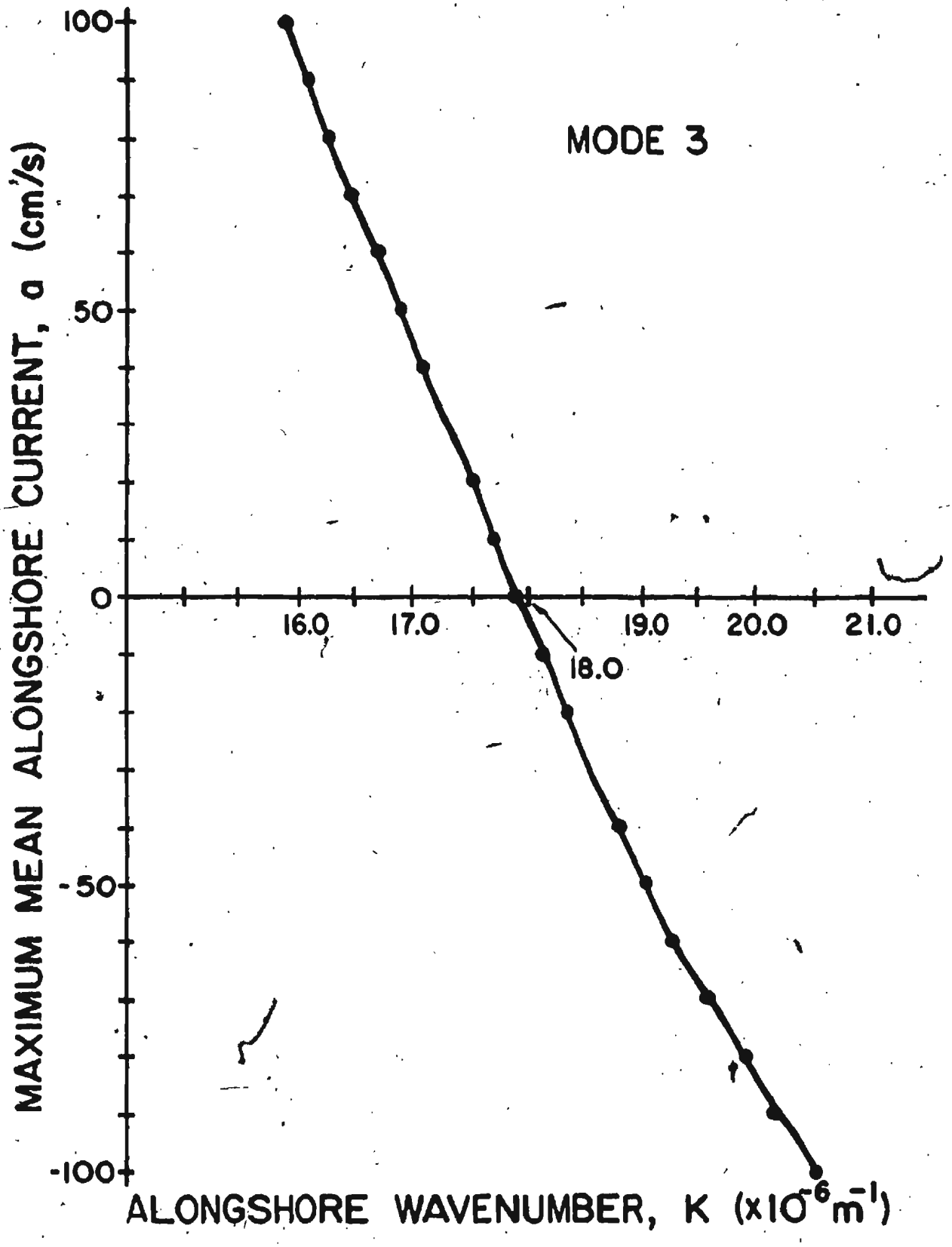

Figure 5.5 Behavior of alongshore wavenumber k for mode three CTW for varying strength and direction of mean alongshore current. Non-dimensional frequency equal to 0.1.

Generally there is a decrease (increase) in wavenumber with an increasingly positive (negative) shear current. The decrease (increase) in wavenumber then implies a increase (decrease) in phase speed. This is exactly what is expected if the wave were advected by the current. However, for mode one a more negative shear current beyond a value of about $-60\ \mathrm{cm\ s^{-1}}$ results in the wavenumber decreasing and hence the phase speed increasing. This is opposite to the effect expected by advection.

The last result may be explained in terms of vorticity though. From barotropic theory it is known that the CTW phase speed is proportional to f [Hsueh, 1980]. Introducing a shear current alters the background potential vorticity of the system from $\frac{f}{H}$ to $\frac{f + \frac{\partial v_o}{\partial x}}{H}$. The contribution of the term $\frac{\partial v_o}{\partial x}$ to the background potential vorticity may become comparable to the contribution of the term f and thereby increase the phase speed of the CTW's. For the particular shear current modeled the term $\frac{\partial v_o}{\partial x}$ is of the order of 25 percent of the term f_o. This can explain how a mean shear current flowing opposite to the wave propagation can increase the phase speed of the wave.

With respect to the Australian experiment, the most realistic choice for the maximum amplitude of the alongshore current is taken as $-50\ \mathrm{cm\ s^{-1}}$. Referring to Figures 5.3, 5.4, and 5.5 the modified phase speed for all three modes is less than the phase speed fo the zero mean current case. For mode one the decrease is only about 1 percent, while for modes two and three it is about 10 percent. In light of the results obtained by Freeland *et al.* [1986] that all three modes were

observed to have phase speeds in excess of those computed theoretically using a model without any shear current, the present model is unable to reproduce those observations. On the other hand, the model results do agree qualitatively with the experimental determination of phase speed by Church *et al.*

CHAPTER SIX

CONCLUSIONS

A numerical method has been presented for the solution of the CTW problem. The method is an extension of present methods in that it allows for the computation of complex or evanescent modes. The ability to compute such modes means that the complete set of CTW mode solutions may be obtained. This in turn implies that, for example, the forced or scattered CTW problem may be indirectly solved.

As outlined in the introduction, this study had three objectives. The first was the presentation of the numerical method. The second was the application of the method to the baroclinic CTW problem. The third was an extension of the baroclinic CTW problem in the presence of a mean alongshore current.

The first objective was met by the presentation of the explicitly shifted inverse power algorithm for the generalized eigenvalue problem. The solution of a problem non-linear in the eigenvalue was accommodated by expanding the solution space to turn the problem into one linear in the eigenvalue. The explicit shift feature allows any particular wavenumber, either real or complex, and corresponding wavestructure of a CTW to be isolated and solved for.

The second objective of the study was met by showing how the introduction of stratification modified the barotropic CTW dispersion relation. It was found that, at a given frequency, CTW mode solutions appear to exist in pairs, either as

a real forward and backward propagating pair or as a complex conjugate evanescent pair. Also, the stratification has the effect of introducing a second zero of group velocity to the dispersion curve for each mode.

The baroclinic dispersion relation for an intermediate stratification indicated that certain real propagating modes were linked to one another through the evanescent modes. For a fixed frequency, the variation of stratification caused such linked modes to transform into one another. The transformation of a real propagating mode into another propagating mode occurred through the process of the real mode becoming complex and then real again. The actual transformation between a real mode and a complex mode always involved a real forward and backward propagating transforming to or from complex conjugate evanescent modes. As well, the transformation was only found to occur at a zero of group velocity of a dispersion curve.

With strong stratification the CTW's propagating modes no longer had any zeros of group velocity and thus no obvious evanescent modes. With increasing stratification the dispersion relation was observed to become more and more non-dispersive. The waves were losing the characteristics of topographic Rossby waves and acquiring those of internal Kelvin waves.

The third objective of this study was the application of the numerical method to the baroclinic CTW problem in the presence of a mean baroclinic alongshore current. An experimental program by Freeland *et al.* [1986] had obtained CTW signals propagating at phase speeds exceeding those computed using a numerical model without a mean current. A modified data analysis by

Church *et al.* obtained the opposite result. The application of the model of Chapter five produced qualitative agreement with Church *et al.* That is, the mean current opposing the flow appears to slow the phase propagation of the lowest three mode CTW's.

APPENDIX A

Derivation of Transformation Equations

The mapping from the (x,z) irregular domain to the (x',z') transformed and regular domain occurs through

$$x' = x, \tag{A.1a}$$

$$z' = T(x)z. \tag{A.1b}$$

The incremental differential relations between the two systems are from (A.1)

$$\frac{\partial x'}{\partial x} = 1, \tag{A.2a}$$

$$\frac{\partial x'}{\partial z} = 0, \tag{A.2b}$$

$$\frac{\partial z'}{\partial x} = \frac{\partial T}{\partial x'}\frac{z'}{T}, \tag{A.2c}$$

$$\frac{\partial z'}{\partial z} = T. \tag{A.2d}$$

Consider the two dimensional pressure function $p(x,z)$. Its numerical value at corresponding points in the two systems must be the same and so

$$p = p(x,z) = p(x',z'). \tag{A.3}$$

Using the chain rule of differential calculus the first derivatives of p are related through

$$\frac{\partial p}{\partial x} = \frac{\partial p}{\partial x'}\frac{\partial x'}{\partial x} + \frac{\partial p}{\partial z'}\frac{\partial z'}{\partial x}, \tag{A.4a}$$

and

$$\frac{\partial p}{\partial z} = \frac{\partial p}{\partial x'}\frac{\partial x'}{\partial z} + \frac{\partial p}{\partial z'}\frac{\partial z'}{\partial z}. \qquad \text{(A.4b)}$$

Applying the relations (A.2) these become

$$\frac{\partial p}{\partial z} = \frac{\partial p}{\partial x'} + \frac{\partial p}{\partial z'}\frac{\partial T}{\partial x'}\frac{z'}{T}, \qquad \text{(A.5a)}$$

and

$$\frac{\partial p}{\partial z} = \frac{\partial p}{\partial z'}T. \qquad \text{(A.5b)}$$

Similarly second derivatives are obtained by a second application of the chain rule yielding

$$\frac{\partial^2 p}{\partial z^2} = \qquad \text{(A.6a)}$$

$$\left(\frac{\partial^2 p}{\partial x'^2}\frac{\partial x'}{\partial z} + \frac{\partial^2 p}{\partial x'\partial z'}\frac{\partial z'}{\partial z}\right)\frac{\partial x'}{\partial z} + \frac{\partial p}{\partial x'}\frac{\partial^2 x'}{\partial z^2} +$$

$$\left(\frac{\partial^2 p}{\partial z'\partial x'}\frac{\partial x'}{\partial z} + \frac{\partial^2 p}{\partial z'^2}\frac{\partial z'}{\partial z}\right)\frac{\partial z'}{\partial z} + \frac{\partial p}{\partial z'}\frac{\partial^2 z'}{\partial z^2},$$

$$\frac{\partial^2 p}{\partial z^2} = \qquad \text{(A.6b)}$$

$$\left(\frac{\partial^2 p}{\partial x'^2}\frac{\partial x'}{\partial z} + \frac{\partial^2 p}{\partial x'\partial z'}\frac{\partial z'}{\partial z}\right)\frac{\partial z'}{\partial z} + \frac{\partial p}{\partial z'}\frac{\partial^2 z'}{\partial z^2} +$$

$$\left(\frac{\partial^2 p}{\partial z'\partial x'}\frac{\partial x'}{\partial z} + \frac{\partial^2 p}{\partial x'^2}\frac{\partial z'}{\partial z}\right)\frac{\partial x'}{\partial z} + \frac{\partial p}{\partial x'}\frac{\partial^2 x'}{\partial z^2},$$

and

$$\frac{\partial^2 p}{\partial x \partial z} = \tag{A.6c}$$

$$\left(\frac{\partial^2 p}{\partial x'^2} \frac{\partial x'}{\partial z} + \frac{\partial^2 p}{\partial x' \partial z'} \frac{\partial z'}{\partial z} \right) \frac{\partial x'}{\partial x} + \frac{\partial p}{\partial x'} \left(\frac{\partial^2 x'}{\partial x \partial x'} \frac{\partial x'}{\partial z} + \frac{\partial^2 x'}{\partial x \partial z'} \frac{\partial z'}{\partial z} \right) +$$

$$\left(\frac{\partial^2 p}{\partial z' \partial x'} \frac{\partial x'}{\partial z} + \frac{\partial^2 p}{\partial z'^2} \frac{\partial z'}{\partial z} \right) \frac{\partial z'}{\partial x} + \frac{\partial p}{\partial z'} \left(\frac{\partial^2 z'}{\partial x \partial x'} \frac{\partial x'}{\partial z} + \frac{\partial^2 z'}{\partial z \partial z'} \frac{\partial z'}{\partial z} \right).$$

With the relations (A.2) these derivatives become

$$\frac{\partial^2 p}{\partial x^2} = \frac{\partial^2 p}{\partial x'^2} \tag{A.7a}$$

$$\frac{\partial^2 p}{\partial x' \partial z'} 2 \frac{\partial T}{\partial x'} \frac{z'}{T} + \frac{\partial^2 p}{\partial z'^2} \left(\frac{\partial T}{\partial x'} \frac{z'}{T} \right)^2 + \frac{\partial p}{\partial z} \frac{\partial^2 T}{\partial x'^2} \frac{z'}{T},$$

$$\frac{\partial^2 p}{\partial z^2} = \frac{\partial^2 p}{\partial z'^2} T^2, \tag{A.7b}$$

and

$$\frac{\partial^2 p}{\partial x \partial z} = \frac{\partial^2 p}{\partial x' \partial z'} T + \frac{\partial^2 p}{\partial z'^2} \frac{\partial T}{\partial x'} z' + \frac{\partial p}{\partial z} \frac{\partial T}{\partial x'}. \tag{A.7c}$$

Thus it is the Equations (A.3), (A.5) and (A.7) which relate a function and its derivatives in the two coordinate systems.

APPENDIX B

Derivation of Finite Difference Forms

The approximation of continuous partial derivatives of the pressure function at a discrete lattice point is obtained by assuming a continuity of derivatives and by carrying out a Taylor's series expansion [Roache, 1985]. Consider the x-direction. The pressure at a point $p_{i+1,j}$ is related to that at $p_{i,j}$ by

$$p_{i+1,j} = p_{i,j} + \left.\frac{\partial p}{\partial x}\right|_{i,j} \Delta x + \tag{B.1}$$

$$\frac{1}{2}\left.\frac{\partial^2 p}{\partial x^2}\right|_{i,j} \Delta x^2 + \frac{1}{6}\left.\frac{\partial^3 p}{\partial x^3}\right|_{i,j} \Delta x^3 + HOT,$$

where HOT represents terms of higher order than Δx^3. Likewise the pressure at a point $p_{i-1,j}$ is

$$p_{i-1,j} = p_{i,j} - \left.\frac{\partial p}{\partial x}\right|_{i,j} \Delta x + \tag{B.2}$$

$$\frac{1}{2}\left.\frac{\partial^2 p}{\partial x^2}\right|_{i,j} \Delta x^2 - \frac{1}{6}\left.\frac{\partial^3 p}{\partial x^3}\right|_{i,j} \Delta x^3 + HOT.$$

Subtracting (B.2) from (B.1) gives

$$p_{i+1,j} - p_{i-1,j} = 2\left.\frac{\partial p}{\partial x}\right|_{i,j} \Delta x + \frac{1}{3}\left.\frac{\partial^3 p}{\partial x^3}\right|_{i,j} \Delta x^3 + HOT. \tag{B.3}$$

Solving for $\frac{\partial p}{\partial x}$ gives

$$\left.\frac{\partial p}{\partial x}\right|_{i,j} = \frac{p_{i+1,j} - p_{i-1,j}}{2\Delta x} + HOT. \tag{B.4}$$

Neglecting terms of higher order than Δx^2 we get the centered finite difference approximation

$$\left.\frac{\partial p}{\partial x}\right|_{i,j} = \frac{p_{i+1,j} - p_{i-1,j}}{2\Delta x}. \tag{B.5}$$

From the same reasoning it follows that

$$\left.\frac{\partial p}{\partial z}\right|_{i,j} = \frac{p_{i,j+1} - p_{i,j-1}}{2\Delta z}. \tag{B.6}$$

The second derivative $\frac{\partial^2 p}{\partial x^2}$ is obtained by adding (B.1) and (B.2) to give

$$p_{i+1,j} + p_{i-1,j} = 2p_{i,j} + \left.\frac{\partial^2 p}{\partial x^2}\right|_{i,j} \Delta x^2 + HOT. \tag{B.7}$$

Solving for $\frac{\partial^2 p}{\partial x^2}$ and neglecting the HOT gives

$$\frac{\partial^2 p}{\partial x^2} = \frac{p_{i+1,j} - 2p_{i,j} + p_{i-1,j}}{\Delta x^2}, \tag{B.8}$$

which is also accurate to second order in Δx. The expression for $\frac{\partial^2 p}{\partial z^2}$ just involves a change in the indices as in

$$\frac{\partial^2 p}{\partial z^2} = \frac{p_{i,j+1} - 2p_{i,j} + p_{i,j-1}}{\Delta z^2}. \tag{B.9}$$

Finally, the cross-derivative term $\frac{\partial^2 p}{\partial x \partial z}$ is approximated by carrying out a double Taylor's series expansion in x and z and keeping a sufficient number of terms such that a second order accuracy in Δx^2 and Δz^2 is maintained. The expression is

$$\frac{\partial^2 p}{\partial x \partial z} = \frac{p_{i+1,j+1} - p_{i+1,j-1} - p_{i-1,j+1} + p_{i-1,j-1}}{4\Delta x \Delta z}. \tag{B.10}$$

APPENDIX C

Verification of Numerical Scheme

The accuracy of the model is tested by comparison of the model results with both analytical and other numerical results. For the special case of a shelf with a flat bottom bounded by a vertical coastal wall and a constant stratification, the baroclinic Kelvin wave solutions are calculable analytically (see Appendix D). The parameters used are $f = 1.0\times10^{-4}\ s^{-1}$, $\omega = 1.0\times10^{-5}\ s^{-1}$, $h = 1000$ m everywhere, $L = 0.0$ km, $D = 20.0$ km, $N^2 = 1.375\times10^{-6}\ s^{-2}$, $nz = 25$, and $nz = 17$. The agreement of the model and the analytical wavenumbers are within one percent for the first mode.

The second verification is for the special case of a shelf profile of exponential form

$$h(x) = h_o\, e^{bx} \qquad x \leq L, \tag{C.1a}$$

$$h(x) = h_o\, e^{bL} = h_1 \qquad x > L. \tag{C.1b}$$

Solutions for this shelf are calculable analytically provided the rigid lid approximation is made and there is no density stratification [Buchwald and Adams, 1968]. Although the model is a baroclinic one, it can simulate a barotropic ocean by setting the buoyancy frequency to a very small number. Comparisons yielded agreement within three percent for the first mode. The parameters used are $f = 1.0\times10^{-4}\ s^{-1}$, $\omega = 3.0\times10^{-5}\ s^{-1}$, $h_o = 21.6$ m, $h_1 = 4900.0$ m, $b = 4.520\times10^{-5}\ m^{-1}$, $L = 120.0$ km, $D = 160.0$ km, $N^2 = 1.0\times10^{-6}\ s^{-2}$, $nz = 25$,

and $nz = 17$.

A third comparison is made for a shelf of linear sloping topography

$$h(x) = h_o + bx \qquad x \leq L, \tag{C.2a}$$

$$h(x) = h_1 \qquad x > L. \tag{C.2b}$$

This time the results are compared with those of a numerical model developed by Brink and Chapman [1985]. The parameters used are $f = 1.0\times10^{-4}\ s^{-1}$, $\omega = 3.15\times10^{-6}\ s^{-1}$, $h_o = 10.0$ m, $h_1 = 4000.0$ m, $b = 3.990\times10^{-2}$, $L = 100.0$ km, $D = 200.0$ km, $N^2 = 1.375\times10^{-6}\ s^{-2}$, $nz = 25$, and $nz = 17$. As with the first comparison the agreement is within one percent for the first mode. The actual numerical results of the comparisons are presented in Table C.1.

Table C.1. Comparison of wavenumber solutions of the numerical model with known analytical solutions and solutions of another numerical model for a mode one CTW.

Type of Comparison	Comparison Wavenumber $\times10^{-6}\ m^{-1}$	Model Wavenumber $\times10^{-6}\ m^{-1}$	Discrepancy Percentage
Analytical Kelvin Wave	26.79	26.92	0.49
Analytical CTW	6.625	6.433	2.98
Numerical CTW	1.000	1.003	0.30

As the scheme used to solve the baroclinic CTW problem is numerical, both the solution eigenvalue k and the corresponding eigenvector $p_{i,j}$ can be expected to become dependent upon the choice for number of horizontal nx and vertical nz grid points. The number of grid points used is $nx = 25$ and $nz = 17$ as used by Brink and Chapman. In the case of a barotropic ocean the eigenvector $p_{i,j}$ does not have any vertical structure and the choice of nz should be irrelevant. However, a baroclinic ocean may require a significant number of grid points in the vertical to resolve the wave structure. As only the first three modes of wave action are investigated in this study the vertical grid resolution with $nz = 17$ is expected to be sufficient. Obviously, increasing the number of horizontal and vertical grid points would improve the accuracy of the model results. Unfortunately, a linear increase in the number of grid points results in a quadratic increase in computational time.

The results of testing the model with various grid spacings for the first three CTW modes are presented in Tables C.2 and C.3. Table C.2 illustrates the effect on a barotropic ocean; Table C.3 illustrates the effect on a baroclinic ocean. The parameters used in Table C.2 are the same as those used in the comparison with the Analytical CTW in Table C.1. Table C.2 indicates that vertical grid spacing has only a minor influence on the solution wavenumber in a barotropic ocean. However, the horizontal spacing is important as a doubling of nx causes the mode three wavenumber to undergo a qualitative change from a real propagating solution to a complex evanescent one. For the baroclinic ocean, the parameters used in Table C.3 are the same as those used in the comparison with the numeri-

cal CTW in Table C.1. It is evident that the effect of grid spacing on wavenumber increases with increasing mode number.

Table C.2. The effect of horizontal and vertical grid spacing on the wavenumber solution for a barotropic ocean for modes one, two, and three.

Mode Number	Number of Horizontal grid Points nx	Number of Vertical Grid Points nz	Solution Wavenumber $\times 10^{-6}$ m^{-1}
1	25	17	6.4327
	50	17	6.4143
	25	34	6.4263
2	25	17	18.601
	50	17	18.992
	25	34	18.548
3	25	17	64.661
	50	17	72.563 + i11.452
	25	34	63.889

Table C.3. The effect of horizontal and vertical grid spacing on a baroclinic ocean for modes one, two, and three.

Mode Number	Number of Horizontal grid Points nz	Number of Vertical Grid Points nz	Solution Wavenumber $\times 10^{-6}$ m^{-1}
1	25	17	1.0028
	50	17	1.0107
	25	34	1.0056
2	25	17	2.8034
	50	17	2.9145
	25	34	2.9820
3	25	17	10.236
	50	17	9.0544
	25	34	11.452

APPENDIX D

Analytical Kelvin Wave Solution

Internal Kelvin waves may exist in a flat-bottom ocean of uniform stratification. For such an ocean the Equations (2.18) become

interior:

$$\frac{\partial^2 p}{\partial x^2} + \frac{\frac{\partial^2 p}{\partial z^2}}{N^2} = k^2 p, \tag{D.1}$$

coast:

$$\sigma \frac{\partial p}{\partial x} = -kp, \tag{D.2}$$

surface and flat bottom:

$$\frac{\partial p}{\partial z} = 0, \tag{D.3}$$

offshore:

$$p \to 0 \quad \text{as} \quad x \to \infty. \tag{D.4}$$

Note that the offshore boundary condition states that the response is trapped at the coast. The partial differential Equation in p complete with boundary conditions is separable in the form

$$p(x,z) = X(x)Z(z). \tag{D.5}$$

Substituting (D.5) into (D.1) gives

$$\frac{\frac{\partial^2 X}{\partial x^2}}{X} - k^2 = -\frac{\frac{\partial^2 Z}{\partial z^2}}{ZN^2} \tag{D.6}$$

Setting each side equal to a separation constant, m^2, results in two ordinary differential Equations

$$\frac{\partial^2 X}{\partial x^2} - (k^2 + m^2)X = 0, \tag{D.7}$$

and

$$\frac{\partial^2 Z}{\partial z^2} + N^2 m^2 Z = 0, \tag{D.8}$$

Consider Equation (D.8) which has the general solution

$$Z(z) = A_z \cos(mNz) + B_z \sin(mNz), \tag{D.9}$$

where A_z and B_z are some unknown constants. Satisfying the surface boundary condition (D.3) requires that $B_z = 0$. Satisfying the bottom boundary condition (D.3) requires that

$$m = -\frac{n\pi}{Nh}, \tag{D.10}$$

where n is an integer. Next consider the Equation (D.7) which has general solution

$$X(x) = A_x e^{-(m^2+k^2)^{\frac{1}{2}}x} + B_x e^{(m^2+k^2)^{\frac{1}{2}}x}, \tag{D.11}$$

where A_x and B_x are some unknown constants. Satisfying the offshore boundary condition requires $B_x = 0$. Satisfying the coastal boundary condition requires

$$k^2 = \frac{n^2\pi^2}{N^2h^2}\left(\frac{\sigma^2}{1-\sigma^2}\right), \tag{D.12}$$

It follows that the respective solutions to the Equations (D.7) and (D.8) are

$$X(z) = A_z\, e^{-\frac{n\pi}{Nh}\left(\frac{1}{1-\sigma^2}\right)^{\frac{1}{2}} z} \tag{D.13}$$

and

$$Z(z) = A_z \cos\left(\frac{-n\pi z}{h}\right). \tag{D.14}$$

The pressure field is calculated as

$$p(x,z) = A_z A_z \cos\left(\frac{-n\pi z}{h}\right) e^{-\frac{n\pi}{Nh}\left(\frac{1}{1-\sigma^2}\right)^{\frac{1}{2}} z} \tag{D.15}$$

The value of the integer parameter n determines the mode number. Also note that N as defined by Eqn (2.16a) is non-dimensionalized by frequency.

References

Bogen, R., 1983: Macsyma Reference Manual. Massachusetts: Massachusetts Institute of Technology Laboratory for Computer Science.

Brink, K.H., 1980: Propagation of barotropic continental shelf waves over irregular bottom topography. *J. Phys. Oceanogr.*, **10** , 765-778.

Brink, K.H., 1982: The effect of bottom friction on low-frequency coastal trapped waves. *J. Phys. Oceanogr.*, **12** , 127-133.

Brink, K.H., and D.C. Chapman, 1985: Programs for Computing Properties of Coastal-Trapped Waves and Wind-Driven Motions Over the Continental Shelf and Slope. Massachusetts: Woods Hole Oceanographic Institute, 99 pp.

Buchwald, V.T., and J.K. Adams, 1968: The Propagation of Continental Shelf Waves. *Proc. Roy. Soc. London*, **A305** , 235-250.

Chapman, D.C., 1983: On the influence of Stratification and Continental Shelf and Slope Topography on the Dispersion of Subinertially Coastally-Trapped Waves. *J. Phys. Oceanogr.*, **13** , 1641-1652.

Church, J.A., H,J. Freeland, and R.L. Smith, 1986: Coastal-Trapped Waves on the East Australian Continental Shelf Part I: Propagation of Modes. *J. Phys. Oceanogr.*, **16** , 1929-1943.

Freeland, H.J., F.M. Boland, J.A. Church, A.J. Clarke, A.M.G. Forbes, A. Huyer, R.L. Smith, R.O.R.Y. Thompson, and N.J. White, 1986: The Australian Coastal Experiment: A Search for Coastal-Trapped Waves. *J. Phys. Oceanogr.*, **16** , 1230-1249.

Gill, A.E., 1982: Atmosphere-Ocean Dynamics. New York: Academic Press, 662 pp.

Gill, A.E. and E.H. Schumann, 1974: The Generation of Long Shelf Waves by the Wind. *J. Phys. Oceanogr.*, **4** , 83-90.

Hamon, B.V., 1962: The Spectrums of Mean Sea Level at Sydney, Coff's Harbour, and Lord Howe Island. *J. Geophys. Res.*, **67** , 5147-5155.

Huthnance, J.M., 1978: On Coastal Trapped Waves: Analysis and Numerical Calculation by Inverse Iteration. *J. Phys. Oceanogr.*, **8** , 74-92.

Hsueh, Y., 1980: Scattering of Continental Shelf Waves by Longshore Variations in Bottom Topography. *J. Geophys. Res.*, **85** , 1147-1150.

Lindzen, R.S., and H.L. Kuo, 1969: A Reliable Method for the Numerical Integration of a Large Class of Ordinary and Partial Differential Equations. *Mon. Weat. Rev.*, **97** , 732-734.

Mitchum, G.T., and Clarke, A.J., 1986: The Frictional Nearshore Response to Forcing by Synoptic Scale Winds. *J. Phys. Oceanogr.*, **16** , 934-946.

Mysak, L.A., 1980: Recent Advances in Shelf Wave Dynamics. *Rev. Geophys. Space Phys.*, **18** , 211-241.

Pond, S., and G.L. Pickard, 1983: Introductory Dynamical Oceanography. Great Britain: Redwood Burn, 329 pp.

Roache, P.J., 1985: Computational Fluid Dynamics. New Mexico: Hermosa Publishers, 446 pp.

Robinson, A.R., 1964: Continental Shelf Waves and the Response of the Sea Level to Weather Systems. *J. Geophys. Res.*, **69** , 367-368.

Stewart, G.M., 1973: Introduction to Matrix Computations. New York: Academic Press, 441 pp.

Wang, D.P. and C.N.K. Mooers, 1976: Coastal-Trapped Waves in a Continuously Stratified Ocean. *J. Phys. Oceanogr.*, **6** , 853-863.

Webster, I.T., 1985: Frictional Continental Shelf Waves and the Circulation Response of a Continental Shelf to the Wind Forcing. *J. Phys. Oceanogr.*, **15** , 855-864.